

Article

# Spatial and Temporal Dynamics of Urban Wetlands in an Indian Megacity over the Past 50 Years

Katja Brinkmann <sup>1,2</sup> , Ellen Hoffmann <sup>1</sup> and Andreas Buerkert <sup>1,\*</sup> 

<sup>1</sup> Organic Plant Production and Agroecosystems Research in the Tropics and Subtropics, Universität Kassel, Steinstrasse 19, D-37213 Witzenhausen, Germany; brinkmann@isoe.de (K.B.); ellen.hoffmann@uni-kassel.de (E.H.)

<sup>2</sup> Institute for Social-Ecological Research (ISOE), Hamburger Allee 45, 60598 Frankfurt/Main, Germany

\* Correspondence: tropcrops@uni-kassel.de; Tel.: +49-5542-98-1228

Received: 7 January 2020; Accepted: 13 February 2020; Published: 17 February 2020



**Abstract:** Asian megacities have attracted much scientific attention in the context of global urbanization, but few quantitative studies analyze wetland transformation in the rural–urban interface. With its rampant growth and transformation from a tree-lined “Garden City” to a busy megalopolis with often-blocked highways and large built-up areas, Bengaluru (Karnataka, S-India) is a good example for assessing how urbanization has led to the acute degradation of wetlands. We therefore investigated long-term land cover and wetland changes from 1965 to 2018 based on an object-based classification of multi-temporal Corona and Landsat images. To quantify and compare the dynamics of open water surfaces and vegetation, we defined the potential wetland areas (PWA) along the rural–urban gradient and linked our analyses to an index describing the degree of urbanization (survey stratification index (SSI)). During the five decades studied, built-up areas in the Bengaluru Urban district increased ten-fold, with the highest growth rate from 2014 to 2018 (+ 8% annual change). Patches of lake wetlands were highly dynamic in space and time, partly reflecting highly variable annual rainfall patterns ranging from 501 mm in 1965 to 1374 mm in 2005 and monsoon-driven alterations in the hydrologic regime. While water bodies and flooded areas shrunk from 64 km<sup>2</sup> in 1965 to 55 km<sup>2</sup> in 2018, in 1965, the total rural wetland area with an SSI > 0.5 was twice as high as in 2018. The rural–urban land cover pattern within potential wetland areas changed drastically during this period. This is reflected, for example, by a four-fold increase in the wetland area with an SSI of 0.3, as compared to a decline by 43% in wetland area with an SSI of 0.8. While, in urban areas, wetlands were mostly lost to construction, in areas with a rural character, open water bodies were mainly transformed into green space. The detected changes in urban wetlands were likely accompanied by ecological regime changes, triggering deteriorations in ecosystem services (ESS) which merit further research.

**Keywords:** lakes; Bengaluru; rural–urban gradient; object-based classification; land cover changes; urbanization

## 1. Introduction

Water bodies and related wetlands provide key ecological functions, such as a habitat for wildlife, groundwater recharge, carbon storage, water regulation [1,2] and other ecosystem services (ESS) that benefit people, such as flood control, fish production, irrigation water, and recreation [3–5]. As such, wetlands are one of the world’s most important natural resources [6]. Despite their importance when it comes to people and the environment, today’s wetlands are under threat due to increasing pressure for human demands, as well as alterations in environmental and climatic conditions [7]. High losses of wetlands occur in many parts of the world [8]. A recent assessment conducted in the context of

the Ramsar Convention on Wetlands revealed that 64% of the world's wetlands have been lost since 1900 [9]. Wetland transformation is particularly critical in metropolitan areas where environmental degradation is a consequence of rapid land use and land cover changes triggered by urbanization. Such changes were recently shown in China in Lianyungang and Beijing [10,11], in South Asia in Bengaluru, India [12] and Colombo, Sri Lanka [13], in Australia in Western Sydney [14], and in Europe in Andalusia, Spain [15] and Uppsala, Sweden [16]. In this context, several authors have indicated that urban wetlands are particularly vulnerable to environmental stressors and ecological transformations are more imminent than in rural wetlands [17,18]. Yet, the role of these habitats as urban social–ecological systems has only been recognized since 2008 as part of the Ramsar discourse [19]. Urbanization and accompanying problems of water provision, waste discharge, space-consuming housing, and industrialization have major effects on ecosystem functions in cities and their associated rural–urban transitional spaces where they affect hydrological and climatic processes such as in Tampa Bay, USA [20] and Lianyungang, China [10].

The processes and speed of wetland losses in urban spaces vary greatly among countries and have, particularly in South Asian cities, also been linked to urban floods, water scarcity, and livelihood losses [21,22]. In many megacities in lower income countries in the Global South, where social inequalities and weak governance aggravate the consequences of environmental pressure, the patterns and trends of urbanization are significantly different from those in post-industrial cities in industrialized countries [23,24], and wetland degradation is more complex [25]. This is particularly true for large urban agglomerations in India, where population growth and city expansion are exceptionally high [26,27] due to rapid industrial and economic development, leading to the high extinction rate of natural habitats, vegetated areas, and wetlands [12,25,28]. Bengaluru (Karnataka State, India), is a prime example in this context and its history and hydrogeological setting was comprehensively reviewed a decade ago [29]. Currently, it is one of the fastest growing megacities in Asia with >10 million inhabitants [30].

In recent decades, the boom of the IT sector led to massive population growth along with drastic land cover changes [31,32]. Complex governance structures, industrial development and the intensification of agricultural land use fueled the encroachment and pollution of water bodies with the consequential loss of natural habitats and ESS [31]. Lack of information on the change dynamics and its drivers as part of a complex social–ecological transformation process [33], limited knowledge about Bengaluru's urban environment, and limited awareness about the role of ESS in people's livelihoods [12], has long hindered the development of effective sustainable management strategies to maintain and potentially restore wetland resources and their multiple functions.

For city planning and effective wetland management, there is a critical need to know the distribution and extent of open surface water and wetlands in space and time and to understand the dynamics and thresholds of ecological change in human-dominated landscapes [16]. Only such information allows for the assessment of competing claims about wetlands [34]. To improve the decision-making process and planning, accurate mapping and monitoring of wetland dynamics is essential [7]. In this context, GIS and remote sensing techniques, with their advantages of synoptic and repeated observations, have become increasingly important tools, providing many advantages compared to time-consuming and costly conventional field survey methods [35–38]. Time series of remote sensing data and satellite image derived vegetation and water indices have been used in many land cover change (LCC) studies focusing on wetland ecosystems [7,11,25,37,39]. The present study exceeds most of the published work in terms of the time scope covered (1965 to 2018); this was achieved by including Corona b/w images in the analysis in addition to various multi-spectral sensors from the Landsat series.

The term wetlands covers a wide variety of different habitats and, although definitions vary, they have much in common [6,40], as they represent the transition between an aquatic and a terrestrial ecosystem [41]. Wetlands are dynamic, both in space and time, and can easily shift from one ecological state to another [8] as a result of annual and seasonal fluctuations in environmental conditions,

such as variation in annual rainfall patterns. Moreover, dynamic and fuzzy spectral boundaries between different wetland types and other land cover categories hamper long-term remote monitoring of wetlands [42,43]. For the identification of water bodies and wetlands, many different remote sensing approaches have been proposed such as supervised [44] and unsupervised classification [45], object-based image analysis (OBIA) [43–45], machine learning algorithms [46], and the spectral water index method [7,47]. The latter is widely used due to its relative high accuracy and its straightforward calculation procedure [48]. The combined use of the advanced classification techniques of multi-temporal imagery and of ancillary information on soils, elevation data or image-derived (water) indices greatly improved wetland classification in recent decades [42]. In particular, OBIA methods, which can incorporate spectral, spatial, textural, and contextual information into the classification process, yield greater accuracies for wetland mapping compared to traditional pixel-based approaches [49]. They are also useful for urban contexts [27].

Some South Asian urban wetland systems have been extensively studied and mapped. Some examples are Kolkata in India [21] and Colombo in Sri Lanka [13]. However, only a few studies have investigated the dynamics and changes in small urban wetlands and (lake) water bodies [50,51], such as those that prevail in the district Bengaluru Urban. For Bengaluru itself, such studies are either restricted to single lakes [52,53] or to a short time series [44,54,55]. So far, no comprehensive long-term study exists on the complex relationships between the structural changes in urbanizing landscapes and the fate of wetlands within them.

To close this knowledge gap, this study aimed at (i) investigating long-term land cover changes (LCC) over the past five decades in Bengaluru using an object-based classification of multi-temporal satellite images combined with ancillary information (water index), (ii) exploring the dynamics of lake wetlands and their dependence on rainfall patterns, (iii) assessing differences of wetland transformation along a rural–urban gradient and (iv) depicting changes within wetland areas in terms of a rural–urban landscape and land cover characteristics. We hypothesized that, in recent decades, urbanization processes and wetland changes were highest in the rural and peri-urban spaces around Bengaluru. The present study therefore attempts, on one hand, to contextualize wetland dynamics with other landscape-related indicators of urbanization and, on the other hand, places a special focus on land cover changes within the potential wetland areas. The latter were identified from the 1965 and 2018 images to create a consistent reference area for the temporal analysis in between.

## 2. Methods

### 2.1. Study Area

Bengaluru, the capital of Karnataka State, is a rapidly growing megacity with a population > 10 million. The study area (2182 km<sup>2</sup>) comprises the Bengaluru Urban district, situated at an altitude between 875 and 940 m a.s.l (Figure 1). The climate is favorable with a mean annual rainfall of approx. 880 mm and a monsoon season lasting from June to October [54]. Due to its large number of open green spaces and a large series of partly interconnected wetlands and water bodies, the city was historically well known as the “Garden City” or “City of Lakes” [12,56,57]. Once a tiny village in the twelfth century [31] it continuously grew through the 16th century when the feudal king Kempegowda of the Vijayanagara empire established the first tanks to meet drinking water needs. The increasingly interconnected tank and lake system was further enlarged throughout the kingdom of the Wodeyars and the Maharajas of Mysore during the 17th and 18th century. It has been documented that the water demand of the growing town eventually became so big that its supply needed to be supplemented by the Cauvery-Arkavathi river system, which ended up becoming almost dry in drought years. Since the colonial period, an increasing number of borewells helped to complement the water supply from Bengaluru’s tank-lake system to satisfy increasing demands for irrigated agriculture, sanitation and drinking water. Excessive exploitation of the aquifer and leaching of waste water make Bengaluru’s future very vulnerable to water scarcity [58,59].

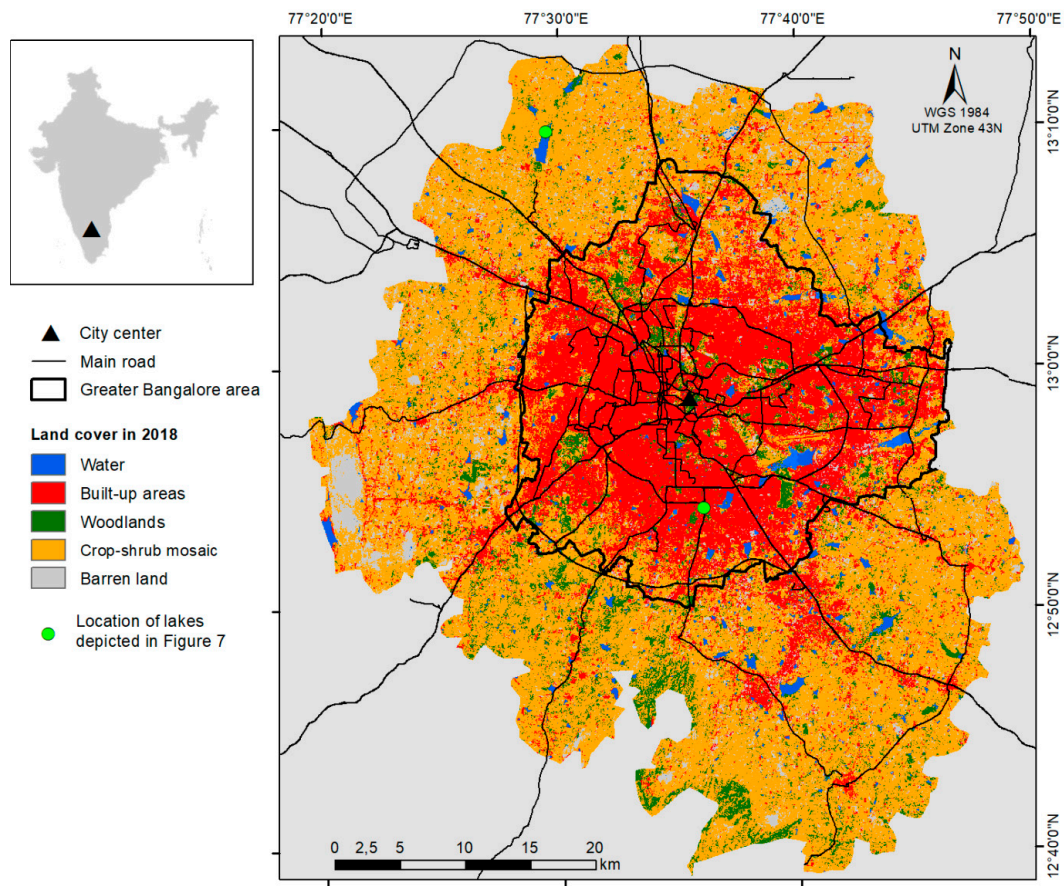


**Figure 1.** Overview of the studied Bengaluru Urban district (S-India) showing the results of the land cover classification for 2018.

Since 1949, urban areas have expanded spatially more than ten times [57], transforming a formerly predominantly rural landscape into an urban metropolis. Today, Bengaluru ranks fourth among India's largest megacities after Delhi, Mumbai and Kolkata [57] with rapid advances in the knowledge-based industries of the information and communication sector [31,60].

For hundreds of years, its hydrological landscape was characterized by small lakes and human-made reservoirs, historically called “katte”, whose water was used for humans and livestock while large open water bodies (“kere”) were used for irrigation of agricultural land [29,61]. The local term “kunte” refers to tanks, which were established “by digging a square cavity into the ground” [62]. Until today, the importance of these water bodies is reflected in many village names. Altogether, more than 200 lakes have been reported within Greater Bengaluru in 2010 [63] and an even larger number of lakes and wetland can be found in the rural hinterlands of the city. Paddy (*Oryza sativa* L.) and ragi (*Eleusine coracana* Gaertn.) are the most important cereal crops cultivated in the area along with other subsidiary crops such as maize (*Zea mays* L.) and various pulses and vegetables. As a consequence of the environmental pressure from population and economic growth, high losses of green space for urban expansion and infrastructure activities have occurred in recent decades [33]. The remaining green space within Bengaluru is diverse and comprises home gardens, forest patches, wooded streets, wetlands, and parks [30,64].

## 2.2. Data Sets and Preprocessing

For time series analysis of land cover and wetland changes from 1965 to 2018, we used panchromatic (b/w) Corona images and Landsat satellite data (Table 1) obtained by the United States Geological Survey (USGS, <https://www.usgs.gov/>). We downloaded cloud-free Landsat image products (L1T), which were

already radiometrically, geographically, and topographically corrected. To assure similar vegetation and surface-hydrological conditions during each year and to minimize bias in the surface water boundaries, the acquisition dates of all Landsat images closely matched. They were all taken during the end of the monsoon period and the beginning of the dry season (December–February). All Landsat images were converted to top-of-atmosphere (TOA) reflectance values using the equations and parameters recommended by [65] and atmospherically corrected using the dark objects approach [66]. For this, we used the Semi-Automatic Classification Plugin within QGIS (ver. 2.18).

**Table 1.** Satellite sensor, date of acquisition, spectral and spatial (m) resolution of the satellite dataset used for land cover change (LCC) analysis of Greater Bengaluru (Karnataka, S-India). Source of Data: U.S. Geological Survey’s Earth Resources Observation and Science.

Satellite (Sensor)	Date of Acquisition	Spectral and Spatial Resolution (m)
Corona KH-4A	10.10.1965	Panchromatic; 2.75
Landsat-5 (TM)	19.01.1988	Band 1-5,7; 28.5
Landsat-5 (TM)	16.01.1993	Band 1-5,7; 28.5
Landsat-5 (TM)	02.02.1999	Band 1-5,7; 28.5
Landsat-5 (TM)	16.12.2004	Band 1-5,7; 28.5
Landsat-5 (TM)	12.01.2009	Band 1-5,7; 28.5
Landsat-8 (OLI TIRS)	10.01.2014	Band 2-7; 28.5
Landsat-8 (OLI TIRS)	21.01.2018	Band 2-7; 28.5

Corona images (KH-4A), which were acquired for the year 1965 and produced by the Central Intelligence Agency (CIA) and the U.S. Air Force [67], depict the earliest data in our time series and had a maximum resolution of 2.75 m at nadir. Due to limited temporal resolution, it was only possible to obtain Corona images for the month of October, depicting the end of the primary rainy season (June–September) and the beginning of the northeast monsoon season. The scanned images were georeferenced using ground control points extracted from recent Google Earth™ images (<https://www.google.com/earth/>). We used easily identifiable landscape features occurring in both image products, such as road intersections, airports, buildings and/or geomorphologic features. Subsequently, the georeferenced images were mosaicked to generate a new image covering the whole study region. All images were clipped to the Bengaluru Urban district area and resampled to the same size (30 m) to match the resolution of the Landsat image using the nearest neighbor method.

Daily rainfall data from 1963 to 2000 from two meteorological stations situated in Bengaluru North and Bengaluru South were employed for the analysis of precipitation effects on lake surfaces. For the period from 2001 to 2019, we used rainfall records from the University of Agricultural Sciences, GKVK station, Bengaluru (<https://www.uasbangalore.edu.in/index.php/research/agromoterology>). Total monthly and annual precipitation was calculated from daily rainfall data for Bengaluru, and used to contextualize the surface area of wetlands and lakes to the climate/weather conditions that prevailed in the observation years.

### 2.3. Classification of Corona and Landsat Images

Initially, the land cover categories occurring in the study area were visually identified based on recent (2018) Google Earth images and field visits. The agricultural land surrounding Bengaluru is characterized by a heterogeneous mosaic of shrubs, trees, annual and permanent crops, fallow fields, and tree plantations. These are all landscape features with high spectral similarities at the beginning of the dry season. We thus tried to reduce classification errors by decreasing the number of land cover categories [68] and using a simplified class for agricultural land including vegetated fallow land with grasses and shrubs. This resulted in the following land cover classes: 1 = water (open water bodies), 2 = hydrophytic vegetation (flooded areas with hydrophytic vegetation), 3 = built-up area (urban cover, including buildings, roads and other asphalted or concreted areas), 4 = woodland (vegetated areas with high tree density), 5 = crop–shrub mosaic (agricultural fields and areas with grass and

shrubs including vegetated fallow fields), 6 = barren land (barren rocks, sparsely vegetated areas). This approach followed the classical classification approach of [69]. It is spatially rather coarse, thereby reflecting (i) the limitations imposed by major differences in the resolution and sensor type of the available satellite images over five decades and (ii) our interest in quantifying and explaining the transformation dynamics of water bodies, associated wetlands and urban development as a function of rural–urban transformation. In our analysis we had to neglect the evident connections of the structural and functional components of human–nature-based urban ecosystem analysis that have been stressed in the HERCULES methodology proposed by [70,71] and were further taken up by [72].

To detect changes in the satellite data, a post-classification comparison approach was applied, which allows the use of heterogeneous data sets by classifying images from different sensors (Corona, Landsat TM and OLI) independently and subsequently comparing the results. Classification was based on an object-based approach within ArcGIS 10.6 (ESRI Inc., Redlands, CA, USA). Image segmentation was performed using the mean shift algorithm [73,74], which is based on a moving window calculating an average pixel value for the determination of pixel combinations for each segment. The segmentation process was applied to the six spectral bands of the Landsat images and the one spectral band of the panchromatic Corona images. Initially, analyses and tests of various parameters for segmentation revealed the best segmentation results using the following parameter settings: 0.1 for shape and 0.5 for compactness. The characteristics of each segment were summarized using the following parameters: spectral detail, spatial detail, and minimum segment size. Training data for the different land cover categories (10–15 per category;  $n = 75$ ) were identified for each segmented image from 2018 and 2014 based on high spatial resolution images provided by Google Earth as well as expert knowledge resulting from on-site field visits in the study area. Due to lacking geographical information, such as historical aerial photographs and data for the inspected years on land cover in the past, we visually redefined the training sites, where necessary. This was done based on the already-known shape and spectral characteristics (color, structure, size) of the different classes using the spectral information of the color–infrared composites of the 1988–2009 Landsat images and the original high-resolution (3 m) Corona image.

After image segmentation and the identification of training sites, a classification with the Random Forest (RF) method using RF models comprising 100 trees and 50 bootstrap samples was applied. The random forest approach is increasingly employed for satellite image classifications, especially for the analysis of wetlands and aquatic habitats [39]. Briefly, RF is based on a machine learning method [75] and works with a collection of decision trees to prevent overfitting. In contrast to classification and regression trees (CART), RF produces multiple decision trees and merges them together to obtain a more accurate and stable prediction. The multiple decision trees of the RF are trained on a bootstrapped sample of the original training data [75].

We added the following segmentation attributes: color, mean, standard deviation, and compactness as classification inputs. Additionally, to improve the detection of water bodies and wetlands, we calculated for each Landsat image the automated water extraction index (AWEI) ([7] Equation (1)) and used it as an ancillary raster dataset in classification. Compared to other indices, such as the normalized difference water index, the normalized modified difference water index, and the water ratio index, the AWEI index yields higher accuracies for water extraction, especially in mountainous areas where classification errors are often a result of terrain-induced shadow effects [7].

$$AWEI = 4 \times (\rho_{blue} - \rho_{SWIR 1}) - (0.25 \times (\rho_{NIR} + 2.75 \times \rho_{SWIR 2})) \quad (1)$$

where  $\rho$  is the reflectance value of spectral bands of Landsat-5 (TM): band 1 (*blue*), band 4 (*NIR*), band 5 (*SWIR 1*), band 7 (*SWIR 2*); or Landsat-8 (OLI TIRS): band 2 (*blue*), band 5 (*NIR*), band 6 (*SWIR 1*), band 7 (*SWIR 2*).

The calculation of the AWEI was impossible for the panchromatic Corona datasets, as well as the automatic detection of all land cover classes due to the lack of spectral information and similar characteristics of ground objects belonging to different classes (barren land, built-up areas, and water

areas). The classification with the RF approach was, therefore, reduced to land cover categories for which automatic detection was feasible, namely woodland, crop–shrub mosaic, and a class combining barren land, water, and built-up areas. During post-processing, this class was refined (see below).

#### 2.4. Post-Processing and Accuracy Assessment

For a post-classification comparison of the classified Landsat and Corona images, it was necessary to improve the image classification of the Corona images and refine the combined class (barren land, water, and built-up areas) using visual interpretation. For this, the land cover categories barren land, built-up, and water including hydrophytic vegetation were detected visually in the original high-resolution Corona images (3m) and manually digitized. The digitized land cover polygons were subsequently transformed into a raster file with a resolution of 30m and merged with the classified Corona image.

An accuracy assessment was conducted using a probability stratified sampling design, as recommended by Olofsson et al. (2014), using the AcATaMa Plugin [76] within QGIS (ver. 2.18; [77]; Appendix A). For the overall sampling size for the accuracy assessment we specified a target standard error for an overall accuracy of 0.01. The resulting sample size using the equation in [78] was  $n = 113$ . Within AcaTaMa, we used random proportional sample allocation for all land cover categories. For the categories with a low proportion, namely water, hydrophytic vegetation and barren land, we randomly allocated 10 additional samples to allow for better accuracy estimates for these land cover categories, resulting in a total number of 123 sample plots for accuracy assessment.

For the 2018 and 2014 classification results, all validation samples were visually classified using high-resolution Google Earth images from 2018 and 2014. Due to the lack of historical geographical data usable for accuracy assessment, the Landsat classification results from 1988 to 1999 were validated based on the original Landsat dataset, displayed as a false color composite. The classification result from 1965 was validated based on the original high-resolution panchromatic image.

For each classified image, a confusion matrix showing the classified data versus the class values of the inspected validation plot was established. Based on this, the reference accuracy (= producers' accuracy, which indicates how well a certain area can be classified), reliability (= users' accuracy, which is the probability that a class on the map represents the category on the ground) and overall accuracy [79] were calculated (Appendix A).

We additionally converted the absolute counts of the sample into the estimated area proportions and calculated the standard errors of the estimated area and the 95% confidence intervals as proposed by [80]. To improve the accuracy estimations, we calculated the quantity disagreement and allocation disagreement, as proposed by [81], as an alternative to the criticized Kappa index. Quantity disagreement is “the amount of difference between the reference map and a comparison map”, whereas allocation disagreement can be considered “as the percentage of classification errors caused by the incorrect spatial allocation of pixels in the classification” [81].

To allow a comparison of the magnitude of land cover changes for the different time periods, we calculated the annual percentage of change using the following formula:

$$C = \frac{A2 - A1}{A1} \times 100 \div (T2 - T1) \quad (2)$$

where C is the annual rate of change (%), A1 is the area of land cover type at time 1 (T1), A2 is the area of land cover type at time 2 (T2).

#### 2.5. Delineation of Potential Wetland Areas (PWA)

Due to the dynamic character of lake wetlands with the seasonal and annual varying extent of open water bodies as a result of hydrologic alterations, correct interpretation of wetland changes using satellite-based time series data is difficult. To overcome this challenge and define a consistent wetland zone for a detailed analysis, we identified the boundaries of potential wetland areas in the study region

and investigated changes in land cover within these areas. The boundaries of all potential wetlands (open water surface and surrounding wetlands with hydrophytic vegetation within a 500 m buffer) were digitized manually on-screen based on Corona images from 1965 and on Google Earth images from 2018. In addition, we used freely available OpenStreetMap (OSM) data (<https://www.openstreetmap.org>; <https://planet.openstreetmap.org>) of open water bodies as a base file, which has been updated and corrected manually using the Google Earth image as a reference. Both areas were combined to produce a shapefile with PWA that existed in 1965 and 2018.

### 2.6. Characterization of the Rural–Urban Gradient and Associated Landscape Morphologies

To analyze wetland changes along the rural–urban gradient, we used a modified index-based approach [82]. Originally developed to facilitate the stratified random sampling of villages for a representative survey (and, thus, named the survey stratification index (SSI)), it was shown that the SSI correlated with certain village and landscape morphologies, such as compact settlements surrounded by fields in rural areas, a heterogeneous mix of different land cover patches in transitional and empty layouts or densely built-up neighborhoods in urban areas. In the rural–urban interface of Bengaluru, these morphologies are distributed in non-linear patterns with pockets of advanced urbanization often associated with major traffic axes or economic infrastructure.

The SSI followed the logic of the urban–rural index [URI], [83] in a simplified manner and used the proportion of built-up areas within a 1 km<sup>2</sup> radius around the village center and its distance to the city center as a proxy for urbanization. Instead of calculating the SSI for buffer zones surrounding settlements, our approach in the present study was to characterize the whole landscape. The study area was, therefore, subdivided in 1 km<sup>2</sup> grid cells to extract the geographical input data for SSI calculations. For each grid, we calculated the proportion of non-built up areas (%; for 1965 and 2018) and the Euclidean distance to the city center (using Vidhana Souda as reference point, according to [82]). Based on the two input parameters, which were normalized to a scale of 0–1, the SSI was calculated for each grid cell using the following equation [82]:

$$SSI = \sqrt{((z_i \text{ distance})(z_i \text{ non-built-up}))} \quad (3)$$

where  $z_i$  is the normalized variable of the Euclidean distance (distance) and the proportion of non-built-up areas (non-built-up).

SSI values thus decrease with increasing urbanization. Roughly, values < 0.3 represent urban areas, values > 0.5 have a rural character, and SSI values ranging from 0.3 to 0.5 represent transitional areas [82]. This simple geographical approach for characterizing the rural–urban gradient does not require statistical data, which are difficult to gather for such a long time series (1965–2018). Nevertheless, it captures the spatially non-linear patterns of different degrees of urbanization.

## 3. Results

### 3.1. Land Cover Changes in Bengaluru Urban

The accuracy assessment for the 2018 image indicated a high accuracy with a quantity disagreement of 5% and allocation disagreement of 0%. For the classification of historical images (1988–2014), the overall accuracy ranged from 93 to 97% (Appendix A). Most of the classification errors were due to quantity disagreement rather than allocation disagreement. The confusion between the land cover categories ‘crop–shrub mosaic’ and ‘woodland’ resulted in a relatively high error of omission. This was mainly due to (fruit) tree plantations within agricultural areas, which were misclassified as woodland.

Overall, the landscape of the Bengaluru Urban district was (73%) and still is (56%) dominated by a crop–shrub mosaic (Figure 1, Table 2, Appendix B). However, the total extent of the crop–shrub mosaic decreased by 23% from 1965 to 2018 and was mainly transformed into built-up land. Although it was not possible to correctly classify cropland automatically, a visual comparison of the historical

Corona images with recent Google Earth images revealed that agricultural fields changed only slightly, and cropland extension was already as high in 1965 as it is today. Built-up areas increased tenfold with the highest expansion rates being between 2004 and 2009 and between 2014 and 2018. Woodland areas have decreased drastically and lost half of their original size over the past 53 years, but there was a complex pattern of conversion and regrowth during the observation period. Until 2009, many areas were deforested, while from 2009 to 2014, the proportion of woodland increased. The deforestation rate was highest in the period from 2014 to 2018, reflecting the intensive construction of new built-up areas.

**Table 2.** Land cover changes (area in km<sup>2</sup>, annual change in %, SE = standard error of area estimates in km<sup>2</sup>, for a detailed accuracy assessment see Appendix A) from 1965 to 2018 in the Bengaluru Urban district, S-India (land cover change data for Greater Bengaluru is summarized in Appendix B).

Year		Water & Hydro. Veg.	Built-up	Woodland	Crop–shrub Mosaic	Barren Land
1965	Area (km <sup>2</sup> )	64.3	52.0	328.3	1590	147.7
	SE (km <sup>2</sup> )	6.9	0.0	0.0	34.8	11.0
1988	Area (km <sup>2</sup> )	51.2	126.4	360.0	1628.7	16.0
	SE (km <sup>2</sup> )	0.0	26.6	34.0	51.7	0.0
	Change (%)	−0.9	6.2	0.4	0.1	−3.9
1993	Area (km <sup>2</sup> )	47.0	171.4	349.2	1595.7	19.0
	SE (km <sup>2</sup> )	10.7	20.9	34.1	45.6	2.7
	Change (%)	−1.6	7.1	−0.6	−0.4	3.8
1999	Area km <sup>2</sup>	57.0	243.4	321.9	1504.2	55.8
	SE (km <sup>2</sup> )	7.6	25.6	22.2	36.2	22.5
	Change (%)	3.5	7.0	−1.3	−1.0	32.3
2004	Area km <sup>2</sup>	46.5	329.0	229.1	1410.3	167.4
	SE (km <sup>2</sup> )	0.0	0.0	22.7	31.8	11.9
	Change (%)	−3.7	7.0	−5.8	−1.2	40.0
2009	Area km <sup>2</sup>	44.9	455.3	167.0	1412.0	103.1
	SE (km <sup>2</sup> )	0.0	18.8	23.3	39.3	0.0
	Change (%)	−0.7	7.7	−5.4	0.0	−7.7
2014	Area km <sup>2</sup>	46.1	449.5	235.4	1302.4	149.0
	SE (km <sup>2</sup> )	6.3	28.5	35.9	43.1	18.2
	Change (%)	0.5	−0.3	8.2	−1.6	8.9
2018	Area km <sup>2</sup>	54.8	592.6	160.6	1222.7	151.6
	SE (km <sup>2</sup> )	4.8	19.5	36.8	42.5	15.2
	Change (%)	4.8	8.0	−7.9	−1.5	0.4
<b>1965 to 2018</b>	<b>Total Change (%)</b>	<b>−14.8</b>	<b>1039.0</b>	<b>−51.1</b>	<b>−23.1</b>	<b>2.6</b>

### 3.2. Dynamics of Lake Wetlands

Patches of lake wetlands were highly dynamic in space and time with displaying increasing and decreasing trends of open water bodies. These likely reflect precipitation patterns and alterations in the monsoon-driven hydrologic regime (Figure 2). However, overall water bodies and flooded areas shrunk from 64 km<sup>2</sup> in 1965 to 55 km<sup>2</sup> in 2018. Losses were highest from 1965 to 1988, increased from 1993 to a transient peak in 1999, and thereafter fluctuated around the 1993 level.

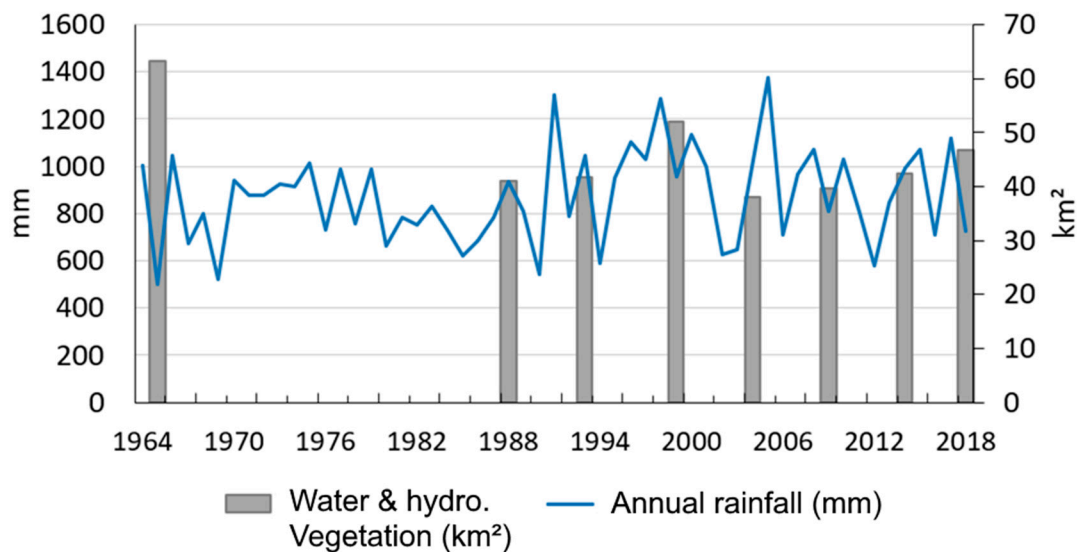


**Figure 2.** Trajectories of annual rainfall (mm) and surface of open water bodies (km<sup>2</sup>) in Bengaluru Urban district (S-India) from 1965 to 2018.

Based on the precipitation data for Bengaluru from 1963 to 2018, the average annual rainfall was 873 mm, which is in good agreement with other sources [54]. The inter-annual variation is high, as is typical for the seasonally dry tropics. The minimum annual precipitation recorded in the observation period was 501 mm in 1965, and the maximum was 1374 mm in 2005 (Figure 2). Among the years chosen for the land cover analysis, 1965 was, thus, the driest year, and most of the rainfall was received in the month of August, while the corresponding satellite picture was obtained in October. All other satellite pictures were taken in or close to the month of January. While the years 1988, 1993, and 2014 were characterized by average precipitation regimes, with rainfall spread over the entire monsoon season, 2004, 2009, and 2018 (with respect to the preceding years) had received higher than average rainfall. On the other hand, 1998 was one of the wettest years recorded (1288 mm). Moreover, it was among a series of six consecutive years (1995–2000) with annual rainfall well above average. This may explain the transient peak in the observed water area in the year 2000. Over the five decades of our study, the water area detected in the observation years reflected the respective rainfall patterns, but generally declined.

The spatial distribution of losses, gains, and unchanged areas of the land cover category “water” for the different observation periods confirmed its very dynamic pattern in space and time (Figure 3). Losses in the first observation period from 1965 to 1988 mainly took place in the periphery of the city in peri-urban and rural landscapes, especially in the north-western part of the city, with high losses in open water for the large Hasaraghatta Lake. From 1993 to 1999, an increase in the groundwater table, likely due to its recharge by high annual precipitation, led to an increase in open water bodies, particularly for the southern part of the study region. From 2014 to 2018, most of the wetland losses occurred in the surrounding area of the old city center and losses in the old city center were highest for the period from 2004 to 2009. Overall, 57% of the detected losses in open water bodies were attributed to their conversion into built-up areas, 6% to a crop–shrub mosaic and 6% to woodland. Gains in open water bodies (lakes, ponds and reservoirs) were found for former woodland (5%) and the crop–shrub mosaic (18%).

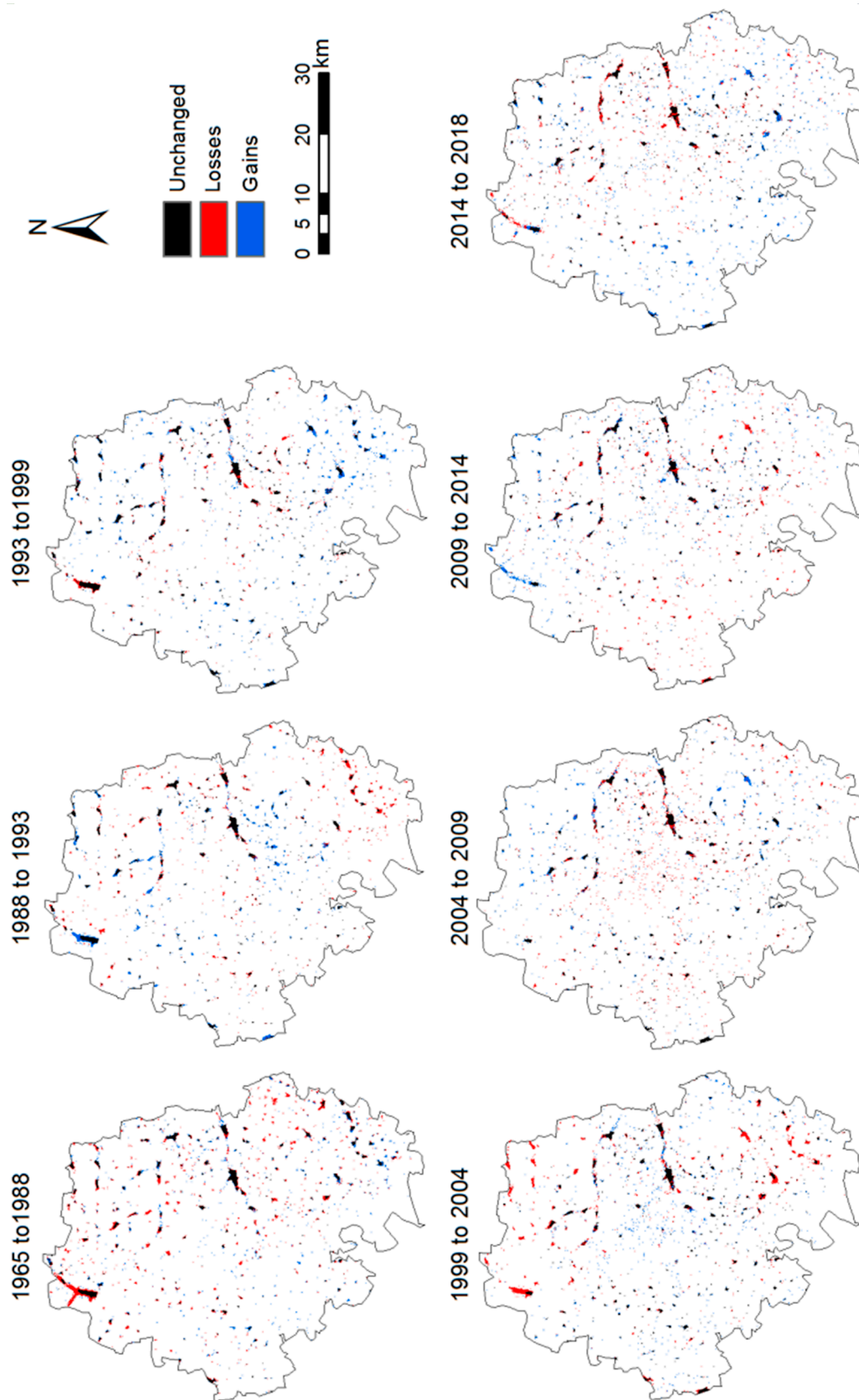


**Figure 3.** Map of losses, gains and unchanged areas of open water bodies for the different observation periods between 1965 and 2018 in the Bengaluru Urban district, S-India.

### 3.3. Changes within PWA along the Rural–Urban Gradient

The delineation of PWA, based on the first and last year of observation, captured a total area of 128 km<sup>2</sup>, distributed over a total of 1118 polygons. The size of the individual PWA ranged from 0.15 to 950 ha. The investigated land cover changes within the potential wetland areas (PWA) confirm the dynamics of lake wetlands in space and time, with likely considerable shifts from one ecological state to another (Figure 4). The land cover categories woodland and crop–shrub mosaic within PWA showed an increasing trend from 1965 to 1993, reflecting the fact that wetland habitats were converted to cropland or green space. While built-up areas consumed 5 km<sup>2</sup> of wetland surface altogether from 1999 to 2018, it devoured as much as 11 km<sup>2</sup> between 1965 and 1999. Water areas were highly variable, resulting from alternating wet and dry periods. In 1999, there was an abrupt rise in open water bodies with a corresponding loss in crop–shrub mosaic. Excess precipitation during 1995 to 2000, with a peak in 1998 (Figure 2), leading to the flooding of many areas surrounding lakes, may explain this transient phenomenon. The effect appears dramatic as only the land cover changes within the PWA are shown in Figure 4. Overall, barren land increased from 1965 to 2018.

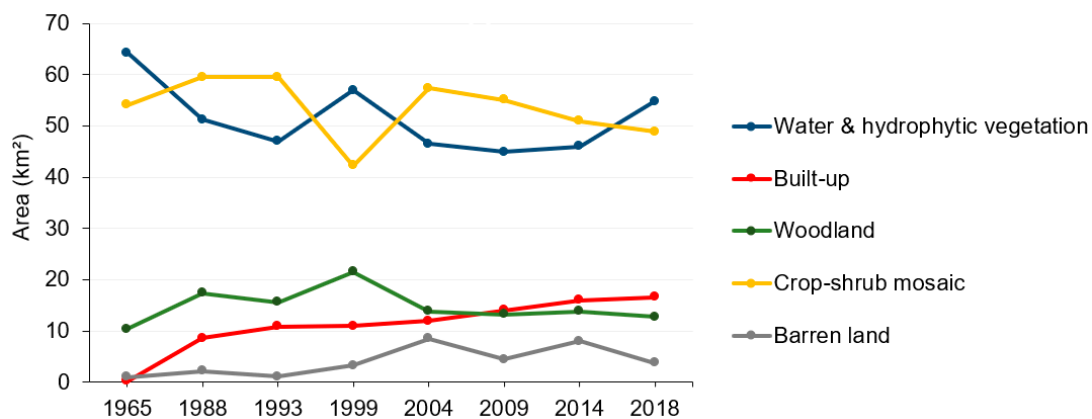


**Figure 4.** Land cover changes from 1965 to 2018 within potential wetland areas (PWA) of the Bengaluru Urban district, S-India.

Changes in lake wetlands and built-up areas over the past five decades were plotted against corresponding SSI values from 2018 to depict the differences along the urban–rural gradient (Figure 5). Water areas within PWA decreased in the urban zone with low SSI values (< 0.3) and were transformed into built-up areas, which is mirrored by the high gains within this land cover category. High vegetation losses in wetlands were found for intermediate SSI values in the transitional zone between urban and rural. In areas with a rural character (SSI > 0.7), the loss of open water bodies was most pronounced, and they were mainly transformed into green space.

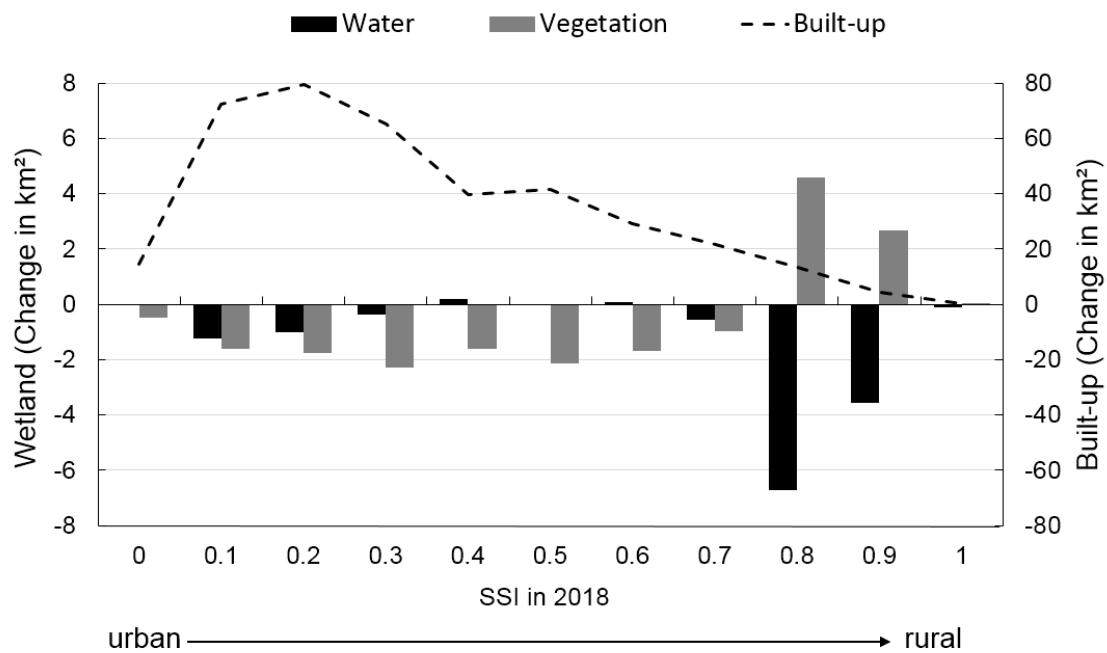


**Figure 5.** Changes (in km<sup>2</sup>) of wetland vegetation and open water bodies (primary y-axis) and built-up areas (secondary y-axis) within PWA from 1965 to 2018 along the rural–urban gradient (SSI values in 2018) in the Bengaluru Urban district, S-India.

### 3.4. Changes in the Rural Urban Characteristics of PWA

The rural–urban characteristics of PWA changed drastically from 1965 to 2018 (Figure 6). In 1965, the rural character with low urbanization (SSI values > 0.5) prevailed, with most lake wetland areas (35 km<sup>2</sup> in total) having an SSI value of 0.8 (Figure 6), this was twice as high as in 2018. In the past five decades, the SSI values within PWA decreased considerably, and only the area with SSI values < 0.3 increased. This indicated that, by 2018, formerly “rural wetlands” had been transformed into wetlands with an urban character (Figure 7).

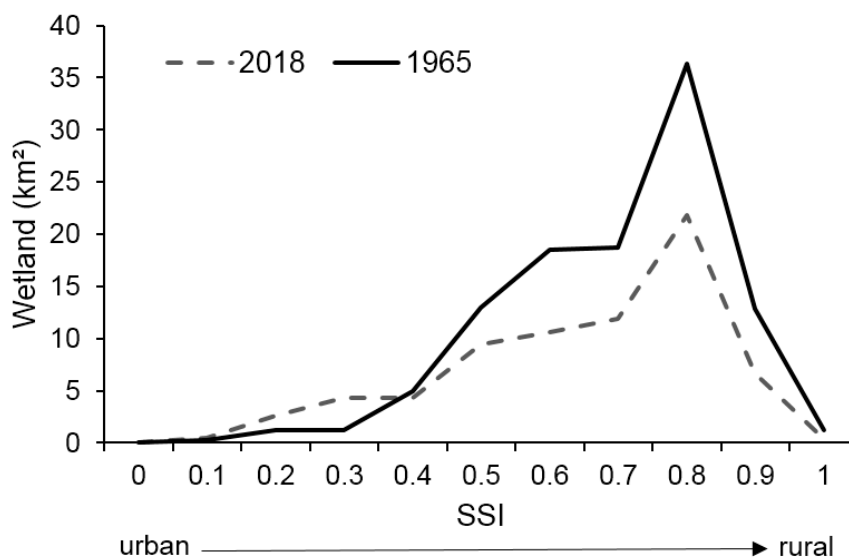


**Figure 6.** Transformation of rural–urban characteristics (survey stratification index (SSI) of Hoffmann et al. (2017) used as a proxy for the degree of urbanization) of lake wetlands (water and vegetated areas in potential wetland areas (PWA)) from 1965 to 2018 in the Bengaluru Urban district, S-India).

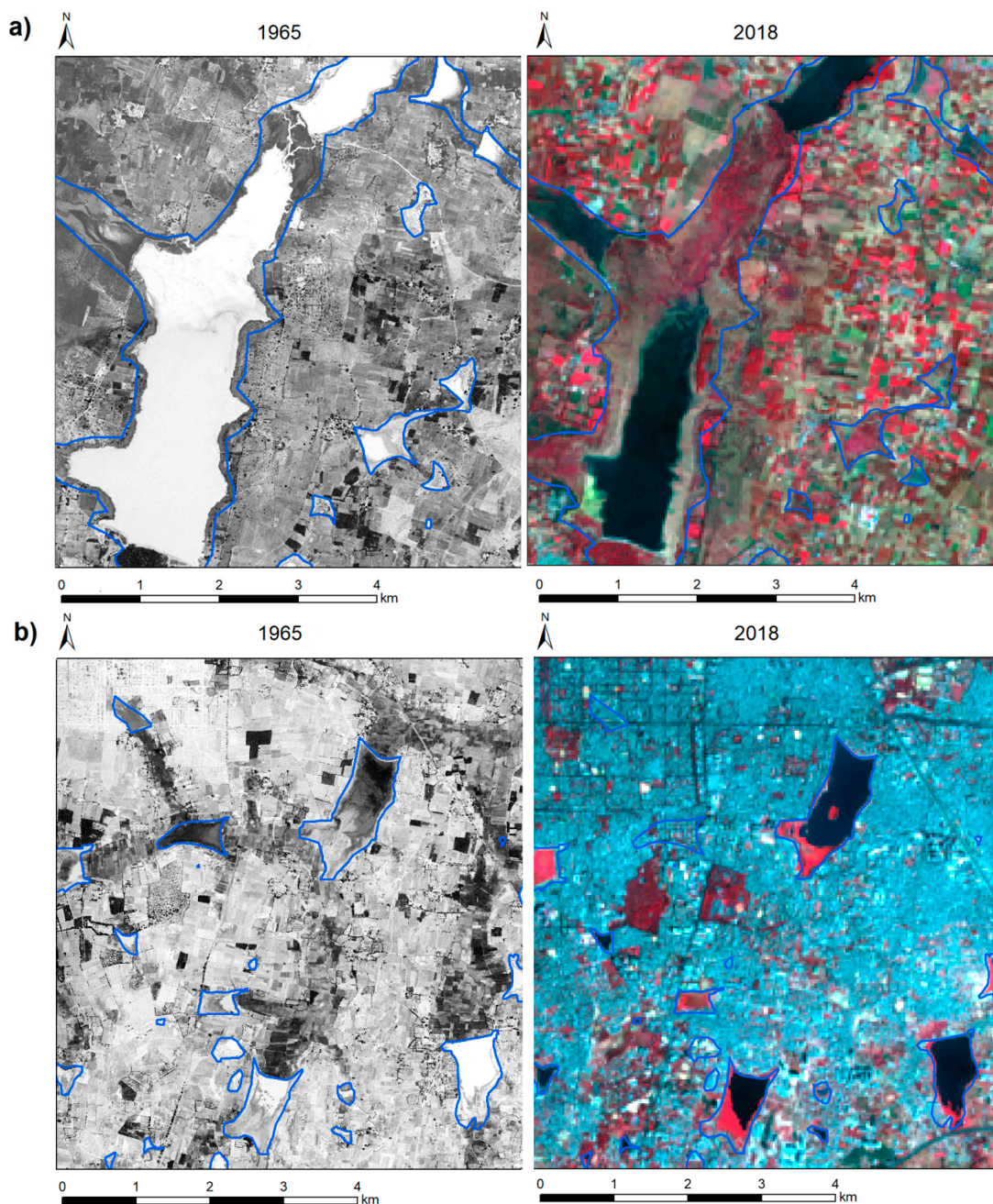


**Figure 7.** Exemplary wetland changes in the Bengaluru urban district from 1965 (Corona image) to 2018 (false color composite of a Landsat-8 image) for (a) rural areas (mean SSI value in 2018 = 0.75) surrounding Hasaraghatta Lake, where wetlands were transformed into green space and (b) urban areas (mean SSI value in 2018 = 0.15), with Agara Lake in the north-east, where wetlands were replaced by built-up areas. The potential wetland area (PWA) is depicted with blue lines.

## 4. Discussion

### 4.1. Land Cover Changes

The summary of our LCC analysis revealed that the most marked change since 1965 was the expansion of built-up areas at the expense of the crop–shrub mosaic, wetlands and woodlands. This is in line with previous studies on LCC in Bengaluru, although the exact change rates may vary due to differences in study design (investigated time periods and spatial scales) and methods (definition of

land cover classes, satellite sensors, spatial and temporal resolution, classification methods, and related misclassification errors). The study in [55] found an increase in built-up areas from 8% in 1973 to 58% in 2012 for Greater Bengaluru with a reduction in water bodies from 3.4% to less than 1%. Although, the inspected time periods differ, we found similar change rates for the increase in built-up areas in Greater Bengaluru (Appendix C) from 7.3% in 1965 to 52.4% in 2009, whereas our data showed a decrease in total water body area from 3% to 2%.

The construction of the Outer Ring Road in 2000 triggered a cascading effect on LCC with the construction of new infrastructure. Many agricultural areas were abandoned, and landowners sold or leased their land for building projects [52]. Although it was not possible to correctly classify cropland automatically, a visual inspection of historical Corona images revealed that cropland extension was already high in 1965, and the total extent of cropland has since shrunk due to massive urbanization. Cropland in the city center was abandoned or transformed into commercial, industrial or residential areas [56,57]. Another group [52] reported that a variety of crops, including rice, ragi, and vegetables were cultivated in the surroundings of Bellandur Lake until recently. Today, most of these fields were either transformed into built-up areas or abandoned, and large parts of this lake are covered with weeds. Some former agricultural land in the city periphery was transformed into permanent crops and tree-plantations. Although agricultural intensification, instead of expansion, predominates in the Bengaluru Urban district, agricultural expansion may play a crucial role in the watershed area of the rural hinterland, which was not inspected in the present study.

We detected an increase in woodland from 2009 to 2014, which is mainly due to large scale conversion of cropland and wetland to plantations of fast-growing trees and patches of parks that were established during the last two decades in the city core area [33]. However, the high proportion of exotic plant species, which dominate the park flora, limits the provision of ESS of these newly established green spaces and may negatively affect native plants and habitats [12].

A very rapid growth in urban areas with new buildings, industries, and infrastructure was detected in our study for the period from 1965 to 1988 and a relatively steady growth during the following observation periods. In the second half of the 1980s, the information technology boom began [60] transforming the former “City of Gardens” into the “Silicon Valley of India”. The high immigration rates pushed population growth and led to increasing pressure on urban wetlands and natural resources [53]. The expansion of built-up areas has mainly taken place in the outskirts of the old city center and in the city periphery along the existing transportation axis due to land scarcity in the city center. This occurred at the expense of croplands, green spaces, and wetlands. This was also reported by [27,33] who found the highest landscape fragmentation and vegetation losses in the city periphery. The former study on urban growth in the 12 largest cities in India revealed that Bengaluru’s growth pattern shows “a transition of mono- to polycentric growth with punctual spatial growth”, with the fastest growth taking place around multiple peripheral areas.

As in many other Indian cities, this urbanization process is barely guided by state policies and results in complex and irregular patterns of growth, with high landscape fragmentation in the periphery, but less urban agglomeration in the city core [27,84]. Such patterns were also found in other Asian cities, such as in Kathmandu [85] and Beijing [86]. The largely unplanned urbanization, or city planning, that follows rather than directs development, results in the degradation of natural ecosystems and resources, including wetlands [27,30,32].

#### *4.2. Wetland Losses along the Rural–Urban Gradient and Its Drivers*

The detected trends in urban wetland losses are similar to those reported for other megacities in South Asia, such as Mumbai, India [87], Kolkata, India [21], Colombo, Sri Lanka [13], and Lianyungang, China [10], where urban wetlands were subjected to rapid human-induced modifications in the late 19th century [13].

In the Bengaluru Urban district, the rural–urban land cover composition within wetlands has changed drastically in the past five decades and, in 1965, the total area of open water bodies in

rural landscapes was twice as high as in 2018. The pattern of wetland changes and conversion was similar to the observed pattern of vegetation losses, with the highest losses in the city periphery [33]. The conversion of bodies of water to built-up areas mainly occurred in the urban ( $SSI < 0.3$ ) and transitional zone ( $SSI > 0.3$  and  $< 0.7$ ), where new residential and commercial areas, as well as industrial parks, have been established. The transition from open water bodies to green spaces and woodland mainly took place in areas with a rural character ( $SSI > 0.7$ ), such as the south eastern and northern region, where natural succession processes in drying lakes took place with the conversion of hydrophytic vegetation stands to shrub and tree habitats (Hasaraghatta Lake, Figure 7a). Many water bodies and wetland areas likely dried out due to disruptions in the connected hydrological drainage network. The remaining wetlands within the city areas are threatened by pollution via domestic and industrial waste, siltation, and the expansion of invasive weed species, which cover large swathes of the lake [57,62,88]. Another study [89] found increasing levels of heavy metal contamination in sediment deposits from the lake beds. Bellandur Lake, which once played a vital role in people's livelihoods [52] has become so loaded with organic pollutants that, in recent years, methane accumulated in it and caused the lake to catch fire several times [90]. Water sample analysis of 305 lakes in the Bengaluru Metropolitan Area (BMA) region revealed that nearly half (44.5%) of the water bodies were contaminated by solid waste from domestic garbage, construction, demolition, and agricultural waste, and 29% of the water bodies suffered from sewage influx [62]. This process of wetland degradation and pollution resulted in irreplaceable losses of valuable ESS, such as biodiversity support, water recharge and nutrient cycling, and contributed to a significant decrease in the city's groundwater table [53].

A comparison of lake losses with other studies is hindered by differences in study design and methods. For the Greater Bengaluru area, a previous study [54] found a decrease in total lake area from 159 (20 km<sup>2</sup>) in 1973 to 107 (10.8 km<sup>2</sup>) in 2002. The authors explored the water surface areas in Greater Bengaluru using several satellite-derived water indices and supervised classification. The results of the different analysis techniques varied between 6.3 and 8.5 km<sup>2</sup> water surface in 2002 versus 5.1 and 7.7 km<sup>2</sup> water surface in 2014. In contrast, we detected 13 km<sup>2</sup> of open water bodies altogether in 2014. These discrepancies can be mainly attributed to the different seasons inspected. Other authors [44] used Landsat data from April, which is the hottest month at the end of the dry season, whereas this information on the inspected season is missing in the study of [54].

The most complete field-and remote sensing-based inventory of lakes was recently conducted by the Centre for Lake Conservation (CLC) team at the Environmental Management & Policy Research Institute (EMPRI). They established a database of water bodies within the Bengaluru Metropolitan Area (BMA) region (1307 km<sup>2</sup>), covering 62% of the Bengaluru Urban district. The study of 1518 water bodies revealed that 10 were created after 1995, while 99 water bodies have vanished. Although the study was based on careful ground truth inventories, there were challenges in the definition and identification of vanished lakes due to the pronounced seasonality of open water bodies [62].

As stated earlier, in the past, the human-made lakes and tanks in Bengaluru and their surrounding were used for fishing, irrigation of cropland, fodder production for cattle [52], drinking water, and domestic uses and, thus, played a key role in people's livelihoods [91]. As a result, many were managed and maintained by local village communities [53]. With the introduction of piped water from the Cauvery River in the 1970s [52] and rapidly growing water extraction from borewells, lakes lost their importance in the supply of fresh water. As a consequence, many lakes were converted for urban land usage [63] and the extensive lake network was transformed into a few isolated and disconnected lakes [57], leading to an increasing risk of flooding in the monsoon season [63]. There was also a shift in people's preferences for lake ESS, from water (irrigation and drinking) and cultural services to recreational services. Such transformations were described in detail by [53] for Agara Lake and by [52] for Bellandur Lake (Figure 7b). The formerly community-based management of lakes was gradually transformed into state management and today, a large number of governmental agencies with overlapping jurisdictions and responsibilities exist, which seem to hamper effective lake management [53].

Like many other cities [10,11,13,14,28], Bengaluru heavily depends on key wetland services, such as filtering nutrients and pollutants, providing wildlife habitats and, in particular, facilitating the regulation of floods during the monsoon season. Frequent flooding in Bengaluru as a result of the increase in the impervious area poses a challenge [62]. Despite recent efforts to protect and restore urban wetlands, and some positive examples of lake restoration by local neighborhood initiatives [92], many lakes continue to be heavily polluted and degraded and/or encroached upon by invasive species [93], whereby the resilience of urban ecosystems heavily depends on the governance of social–ecological system resources as a result [94]. Weak governance is certainly another important driver of wetland change, next to activities including infrastructural development, construction activities, and industrial and agricultural use [10]. However, climatic and environmental conditions are similarly important and hamper the investigation into human-induced wetland changes, especially as many lakes are seasonal with the existence of open water bodies being restricted to half the year. Our time series analysis also highlights the lake dynamics in space and time due to fluctuations in water levels and inundation, which have varied substantially through time in response to precipitation and evapotranspiration.

#### 4.3. Methods Used for the Identification of Wetland Changes

The complexity of the human-made landscapes in and around megacities with highly variable spectral signatures in space and time leads to several challenges in remote sensing-based time series analysis [32], particularly for the long-term monitoring of wetland cover [20,42]. Within the Bengaluru Urban district, the extension of lake wetlands is highly variable, resulting from alternating wet and dry periods and varying water permanency (ephemeral, temporal, seasonal, semi-permanent, and permanent [62]). As a consequence, these “transitional” habitats may rapidly shift from one ecological state to another irrespective of climatic conditions and land use activities affecting the water regime. Our results (Figure 1) show a relation between the open water area detected in the satellite images and the precipitation around the observation date. Seasonal fluctuations are often accompanied by a gradual transformation from aquatic lake ecosystems to terrestrial ecosystems due to drying and the lack of water inflow [8]. Both processes, seasonal fluctuations and autogenic, as well as allogenic, successions, hamper the documentation of human-induced long-term changes in wetlands. Further constraints in satellite-based time series analysis are (i) fluctuating water levels and the accompanied changes in the spectral reflectance of vegetation, (ii) confusion caused by periphyton, which can form large floating vegetation masses, especially during the dry season, and (iii) difficulties in separating overlapping signatures with other (upland) land cover types [42]. These challenges increase misclassification errors, which may accumulate in time series analyses [95,96]. We tried to overcome some of these challenges by using simplified land cover categories and placed the focus on changes in open water bodies and green space in defined potential wetland areas.

Although our classification technique, based on OBIA and using an improved water index (AWEI) as the ancillary information, resulted in relatively high overall accuracies (> 90%), several constraints hindered effective image classification. One directly refers to the limitations of the accuracy assessment of the 1965–2009 images in the current study due a lack of historical ground surveys and geographical reference data, such as high-resolution images or aerial photographs. Furthermore, there is always an interpreter uncertainty in the reference classification; however, this is very difficult to estimate for historical datasets, for which a “gold standard” of truth is lacking [80]. We, therefore, need to take into account the fact that such errors may lead to error accumulation within a post-classification comparison approach [96]. However, due to the simplified land cover categories that we used in classification, the study’s interpreter bias is likely low.

During post-processing, visual on-screen interpretation was necessary for the classified 1965 image to reclassify the water, barren land, and urban areas. Urban areas were easy to detect on the high-resolution Corona image due their textural characteristic, whereas reasonable thresholds between water areas and barren land were difficult to define due to their spectral similarities and their

homogenous texture. Consequently, some of the observed wetland and land cover changes may be over and/or underestimated, especially between 1965 and 1988. Although the visual change detection is hampered by the interpreter bias and may be difficult to replicate [80,96], it is also known that visual interpretations frequently result in a more accurate image interpretation compared to automatic classification approaches, due to the simultaneous processing of texture, color tones, and geometric features [97].

Further constraints in image classification resulted from the complexity of natural wetland conditions on the ground. Many wetlands are only flooded at certain times during the year and a careful selection of the study season is, therefore, a critical issue in time series analysis. To better identify (temporary) lake wetlands, it is recommended to use satellite images acquired at peak water level [42]. However, due to a lack of cloud-free data for the monsoon season, we selected Landsat datasets depicting the beginning of the dry season. In this way, we minimized the impact of seasonal variation and tried to make sure that water levels in lakes were still relatively high. Nevertheless, the significant seasonality of the lake's inundation area hampered detection of lake losses, as well as a comparison with other remote sensing-based studies on wetland changes in Bengaluru. Inconsistencies in estimated wetland and lake areas and their change rates in different reports and scientific studies may be attributed to these issues. Reliable estimations on lake disappearance will need to be validated with high-resolution satellite data and verified during ground visits. In addition, the actual dynamics (changes in size) of individual lakes and wetlands in response to rainfall patterns at a finer time resolution would merit further investigation. This should be accompanied by vegetation surveys to investigate the degree of succession and assess if possible regime shifts from an aquatic ecosystem to a terrestrial vegetation type are irreversible or not.

Visualizing the wetland dynamics as a function of the SSI is a novel approach to analyzing and depicting the interrelations between the described land cover changes and other rural–urban transition processes and their impact on specific ecosystem services. Few studies actually define and quantify parameters related to this nexus. In an earlier example [98], researchers explored biodiversity within 21 pre-defined wetland areas in the Netherlands, measured as the number of endangered bird and angiosperm species in the context of rural–urban landscape characteristics. The authors used indicators such as areas of built-up land, population density, road density, open water area, agricultural land use, intensity of fertilizer use, and distance to the city of Amsterdam. They showed significant co-variance between these urbanization-related parameters as well as negative effects of increasing urbanization on plant biodiversity, but not on bird biodiversity. They further concluded that agriculture and urbanization could not be separated as causal agents of wetland transformations, but that a distinct gradient in population density was superimposed with two other separate gradients, thus creating a more complex spatial pattern and multi-causal variability. The SSI used in the present study integrates some of the same parameters, thus allowing us to better correlate the observed wetland dynamics with non-linear rural–urban transition patterns.

Another comprehensive approach allowed researchers to map, quantify, and characterize wetlands in the metropolitan area of Sydney, Australia [14]. Here, the land in the area surrounding the wetlands was used as a proxy for a rural–urban gradient, assuming a succession from native ecosystems, to agricultural and then urban landscapes. Based on data pooled from 1999 to 2006 (and covering ca. 5000 water bodies in three size classes, from less than 1000 to more than 2000 m<sup>2</sup>) they showed a discontinuous distribution in the size, density and shape of wetlands, with typical features for rural, transitional and urban areas, which resonates with the conclusions drawn in our paper (Figure 5).

## 5. Conclusions

Our findings yield important insights into the dynamics of lake wetlands in the rural–urban interface of Bengaluru using a combination of OBIA based on spectral bands and an improved water index as ancillary information to detect lakes and wetland areas with high precision and the SSI approach to analyze and depict the interrelations between the described land cover changes and other

rural–urban transitions. Despite increasing efforts to protect and restore urban wetlands, many continue to be used as dumpsters, a process that particularly affects the city periphery, which has been undergoing rapid urbanization in recent decades due to land scarcity in the city center. The large-scale urbanization and continued losses of green space and water bodies poses a great challenge for city planning in Bengaluru, especially for the future availability of water, which is going to be an increasingly important factor affecting city development. The analysis presented in our paper highlights the potential for integrated approaches to understand the consequences of rural–urban transformation on sustainable development of an Indian megacity. It is, thus, equally important for policy makers and conservation environmentalists to understand these consequences as well. To identify effective options in urban wetland management, city planners may need to monitor and assess the effectiveness of current and past practices and pay attention to the spatial allocation of restoration activities in the social–ecological context that governs the past, present, and future of each lake.

In the past five decades, in Bengaluru, regime shifts in the use of urban wetlands were accompanied by considerable changes in ESS benefits and people’s valuations of ESS. A major contributor to this was the change from community-based wetland management to centralized management under state control. The related failures in wetland governance have aggravated the already alarming environmental situation. To restore and optimize key wetland functions and services, there is an urgent need for further research on the resilience of wetland ecosystems, combining the different ecological, socio-economic, cultural, and institutional components of the complex urban social–ecological systems governing them.

**Author Contributions:** Idea and conceptualization, A.B., K.B.; methodology, K.B.; writing—original draft preparation, K.B. and E.H.; Writing—review and editing, E.H. and A.B.; funding acquisition, A.B.; supervision, A.B. All authors have read and agreed to the published version of the manuscript.

**Funding:** This research was supported by the German Science Foundation (DFG) as part of FOR2432/2 “Social-Ecological Systems in the Indian Rural-Urban Interface: Functions, Scales, and Dynamics of Transition” (Grant No. BU1308/13-2).

**Acknowledgments:** The authors would like to thank PR Sheshagiri Rao, Vice President (Agronomy), Natural Remedies Pvt. Ltd, Veerasandra Industrial Area, Bangalore, India and K.N. Ganeshiah, University of Agricultural Sciences (UAS), GKVK Campus for kindly providing access to long term rainfall data of Bangalore.

**Conflicts of Interest:** The authors declare no conflict of interest.

## Appendix A Accuracy Assessment

Summary of the accuracy assessment of the Landsat images used to examine LCC in the Bangalore Urban district (S-India). Users’ accuracy (UA) (%), producers’ accuracy (%).

Land Cover Class	2018		2014		2009		2004		1999		1993		1988		1965	
	UA	PA														
Water	90.0	100.0	100.0	100.0	100.0	100.0	100.0	100.0	100.0	100.0	100.0	77.8	100.0	100.0	88.9	100.0
Hydrophytic vegetation	100.0	100.0	100.0	88.9	100.0	100.0	100.0	100.0	100.0	66.7	100.0	100.0	100.0	100.0	100.0	100.0
Built-up	100.0	93.1	95.6	91.7	95.8	100.0	100.0	100.0	84.6	100.0	81.8	100.0	66.7	100.0	100.0	100.0
Woodland	100.0	71.4	80.0	85.7	94.1	88.9	93.8	93.8	90.0	100.0	95.8	88.5	90.0	90.0	88.9	88.9
Crop–shrub mosaic	92.9	100.0	96.8	95.2	96.8	96.8	98.5	96.9	98.7	96.3	95.8	97.2	96.1	93.7	95.8	95.8
Barren land	100.0	100.0	81.8	100.0	100.0	100.0	92.8	100.0	100.0	100.0	85.7	100.0	100.0	100.0	100.0	83.3
Overall accuracy (%)	95.1		93.5		96.4		97.3		95.9		94.3		93.5		94.3	
Quantity disagreement (%)	4.9		2.4		0.8		0.8		3.3		3.2		1.6		0.8	
Allocation disagreement (%)	0		4.1		2.4		1.6		0.8		2.4		4.9		4.9	

Error matrices of the land use classes for 2018, 2014, 2009, 2004, 1999, 1993 and 1988 in the Bangalore Urban district (S-India). The standard error of area estimates (km<sup>2</sup>) and 95% confidence interval were calculated as proposed by Olofsson et al. (2014) based on an area-based error matrix. Class abbreviations: 1 = water; 2 = hydrophytic vegetation; 3 = built-up, 4 = woodland, 5 = crop–shrub mosaic, 6 = barren land.

Error matrix for 2018									
Classified	1	2	3	4	5	6	SUM	Total Area (km <sup>2</sup> )	Stratum Weight (WI)
1	9	0	1	0	0	0	10	48.0	0.022
2	0	10	0	0	0	0	10	6.8	0.003
3	0	0	27	0	0	0	27	592.6	0.272
4	0	0	0	10	0	0	10	160.6	0.074
5	0	0	0	4	52	0	56	1222.7	0.560
6	0	0	1	0	0	9	10	151.6	0.069
<b>SUM</b>	<b>9</b>	<b>10</b>	<b>29</b>	<b>14</b>	<b>52</b>	<b>9</b>	<b>123</b>	<b>2182.34</b>	<b>1.000</b>
<b>Standard error of area estimates (km<sup>2</sup>)</b>	4.8	0.0	19.5	36.8	42.5	15.2			
<b>95% Confidence interval (km<sup>2</sup>)</b>	9.4	0.0	38.2	72.1	83.2	29.7			

Error matrix for 2014									
Classified	1	2	3	4	5	6	SUM	Total Area (km <sup>2</sup> )	Stratum Weight (WI)
1	4	0	0	0	0	0	4	27.6	0.013
2	0	8	0	0	0	0	8	18.9	0.009
3	0	0	22	0	1	0	23	449.5	0.206
4	0	1	0	12	2	0	15	235.4	0.108
5	0	0	0	2	60	0	62	1302.4	0.596
6	0	0	2	0	0	9	11	149.0	0.068
<b>SUM</b>	<b>4</b>	<b>9</b>	<b>24</b>	<b>14</b>	<b>63</b>	<b>9</b>	<b>123</b>	<b>2182.3</b>	<b>1.000</b>
<b>Standard error of area estimates (km<sup>2</sup>)</b>	0.0	6.3	28.5	35.9	43.1	18.2			
<b>95% Confidence Interval in km<sup>2</sup></b>	0.0	12.3	56.05	70.4	84.5	35.6			

Error matrix for 2009									
Classified	1	2	3	4	5	6	SUM	Total area (km <sup>2</sup> )	Stratum Weight (WI)
1	7	0	0	0	0	0	7	36.1	0.017
2	0	5	0	0	0	0	5	8.8	0.004
3	0	0	23	0	1	0	24	455.3	0.209
4	0	0	0	16	1	0	17	167.0	0.077
5	0	0	0	2	60	0	62	1412.0	0.647
6	0	0	0	0	0	8	8	103.1	0.047
<b>SUM</b>	7	5	23	18	62	8	123	2182.3	1.000
<b>Standard error of area estimates (km<sup>2</sup>)</b>	0.0	0.0	18.8	23.3	39.3	0.0			
<b>95% Confidence Interval in km<sup>2</sup></b>	0.0	0.0	37.2	45.7	79.7	0.0			

Error matrix for 2004									
Classified	1	2	3	4	5	6	SUM	Total area (km <sup>2</sup> )	Stratum Weight (WI)
1	8	0	0	0	0	0	8	40.2	0.018
2	0	4	0	0	0	0	4	6.3	0.003
3	0	0	16	0	0	0	16	329.0	0.151
4	0	0	0	15	1	0	16	229.1	0.105
5	0	0	0	1	64	0	65	1410.3	0.646
6	0	0	0	0	1	13	14	167.4	0.077
<b>SUM</b>	8	4	16	16	66	13	123	2182.3	1.000
<b>Standard error of area estimates (km<sup>2</sup>)</b>	0.0	0.0	0.0	22.7	31.8	11.9			
<b>95% Confidence Interval in km<sup>2</sup></b>	0.0	0.0	0.0	44.6	62.4	23.4			

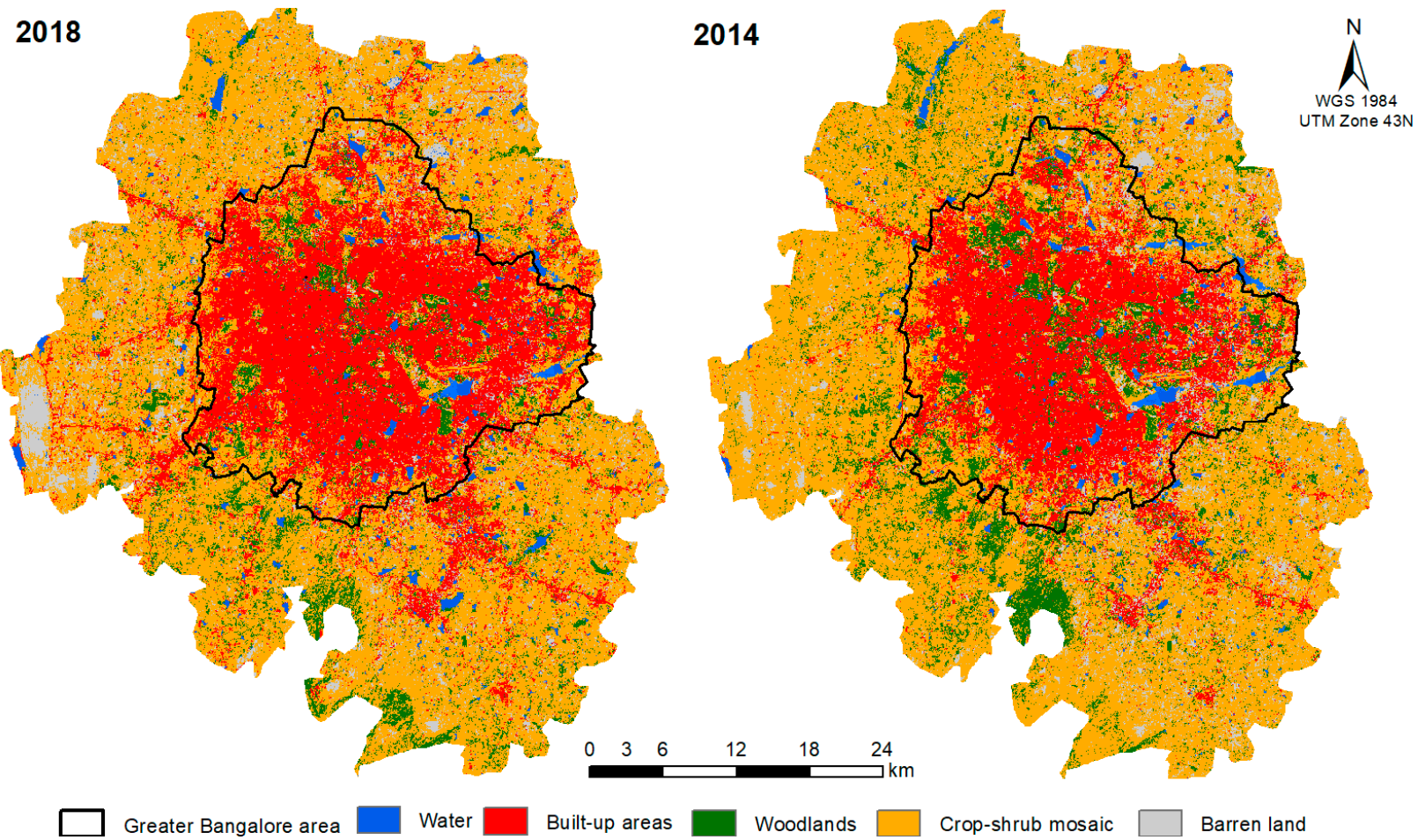
Error matrix for 1999									
Classified	1	2	3	4	5	6	SUM	Total area (km <sup>2</sup> )	Stratum Weight (WI)
1	8	0	0	0	0	0	8	53.0	0.024
2	0	2	0	0	0	0	2	5.0	0.003
3	0	0	11	0	1	1	13	243.4	0.112
4	0	0	0	18	2	0	20	321.9	0.148
5	0	1	0	0	77	0	78	1504.2	0.688
6	0	0	0	0	0	2	2	55.8	0.026
<b>SUM</b>	8	3	11	18	80	2	123	2182.3	1.000
<b>Standard error of area estimates (km<sup>2</sup>)</b>	0.0	7.6	25.6	22.2	36.2	22.5			
<b>95% Confidence Interval in km<sup>2</sup></b>	0.0	14.9	50.2	43.4	70.9	44.2			

Error matrix for 1993									
Classified	1	2	3	4	5	6	SUM	Total area (km <sup>2</sup> )	Stratum Weight (WI)
1	7	0	0	0	0	0	7	42.9	0.020
2	0	2	0	0	0	0	2	4.1	0.002
3	1	0	9	0	1	0	11	171.4	0.079
4	0	0	0	23	1	0	24	349.2	0.160
5	0	0	0	3	69	0	72	1595.7	0.731
6	1	0	0	0	0	6	7	19.0	0.009
<b>SUM</b>	9	2	9	26	71	6	123	2182.3	1.000
<b>Standard error of area estimates (km<sup>2</sup>)</b>	10.7	0.0	20.9	34.1	45.6	2.7			
<b>95% Confidence Interval in km<sup>2</sup></b>	21.0	0.0	41.0	66.9	89.4	5.3			

Error matrix for 1988									
Classified	1	2	3	4	5	6	SUM	Total area (km <sup>2</sup> )	Stratum Weight (WI)
1	6	0	0	0	0	0	6	46.9	0.022
2	0	2	0	0	0	0	2	2.3	0.001
3	0	0	4	0	2	0	6	126.4	0.058
4	0	0	0	27	3	0	30	360.0	0.165
5	0	0	0	3	74	0	77	1628.7	0.747
6	0	0	0	0	0	2	2	16.0	0.007
<b>SUM</b>	6	2	4	30	79	2	123	2182.3	1.000
<b>Standard error of area estimates (km<sup>2</sup>)</b>	0.0	0.0	26.6	34.0	51.7	0.0			
<b>95% Confidence Interval in km<sup>2</sup></b>	0.0	0.0	52.2	66.7	101.3	0.0			

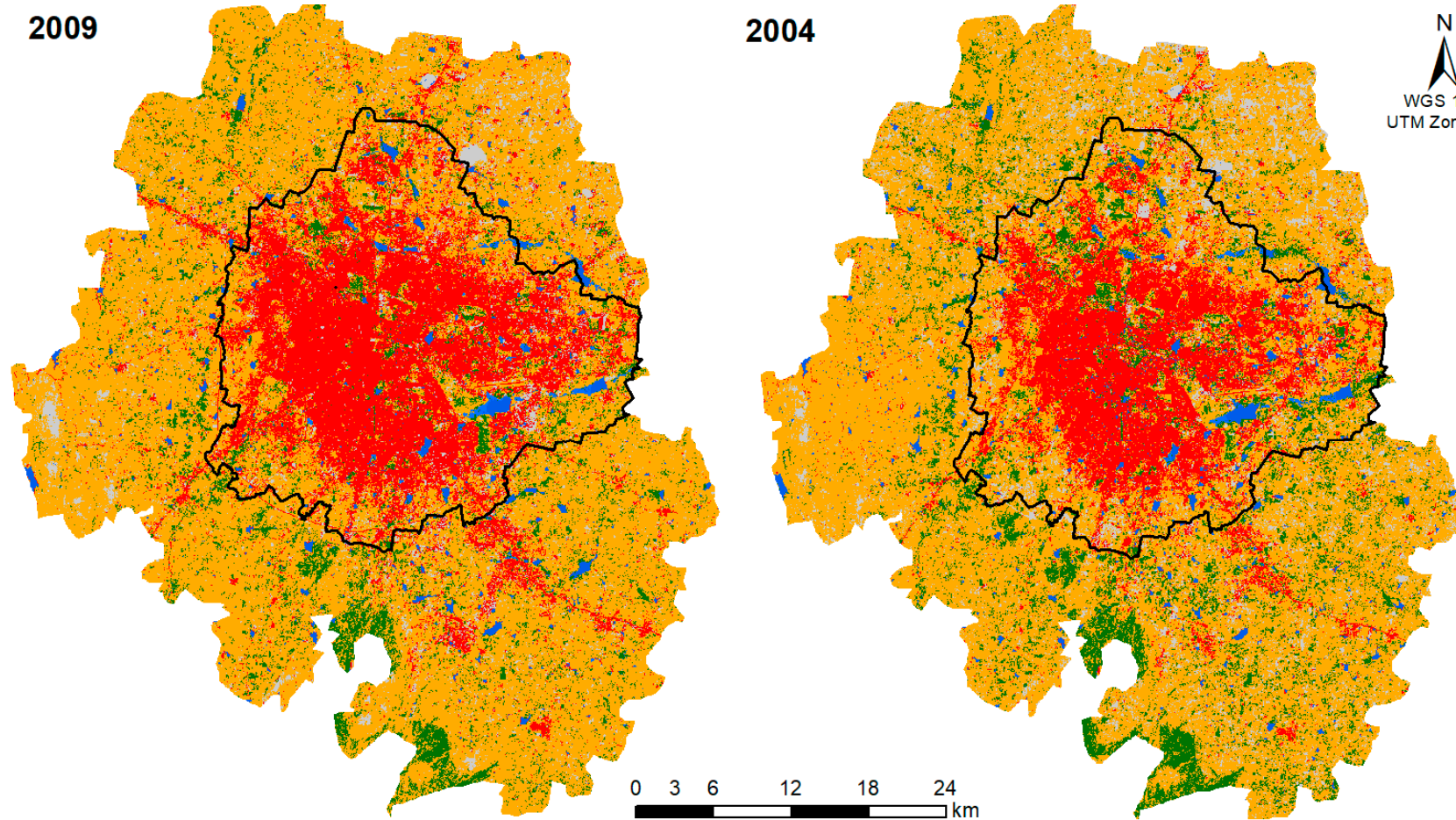
Error matrix for 1965									
Classified	1	2	3	4	5	6	SUM	Total area (km <sup>2</sup> )	Stratum Weight (WI)
1	8	0	0	0	0	1	9	62.2	0.029
2	0	4	0	0	0	0	4	2.1	0.001
3	0	0	6	0	0	0	6	52.0	0.024
4	0	0	0	24	3	0	27	328.3	0.150
5	0	0	0	3	69	0	72	1590.0	0.729
6	0	0	0	0	0	5	5	147.7	0.068
<b>SUM</b>	8	4	6	27	72	6	123	2182.3	1.000
<b>Standard error of area estimates (km<sup>2</sup>)</b>	6.9	0.0	0.0	34.8	45.7	11.0			
<b>95% Confidence Interval in km<sup>2</sup></b>	13.5	0.0	0.0	68.1	89.6	21.5			

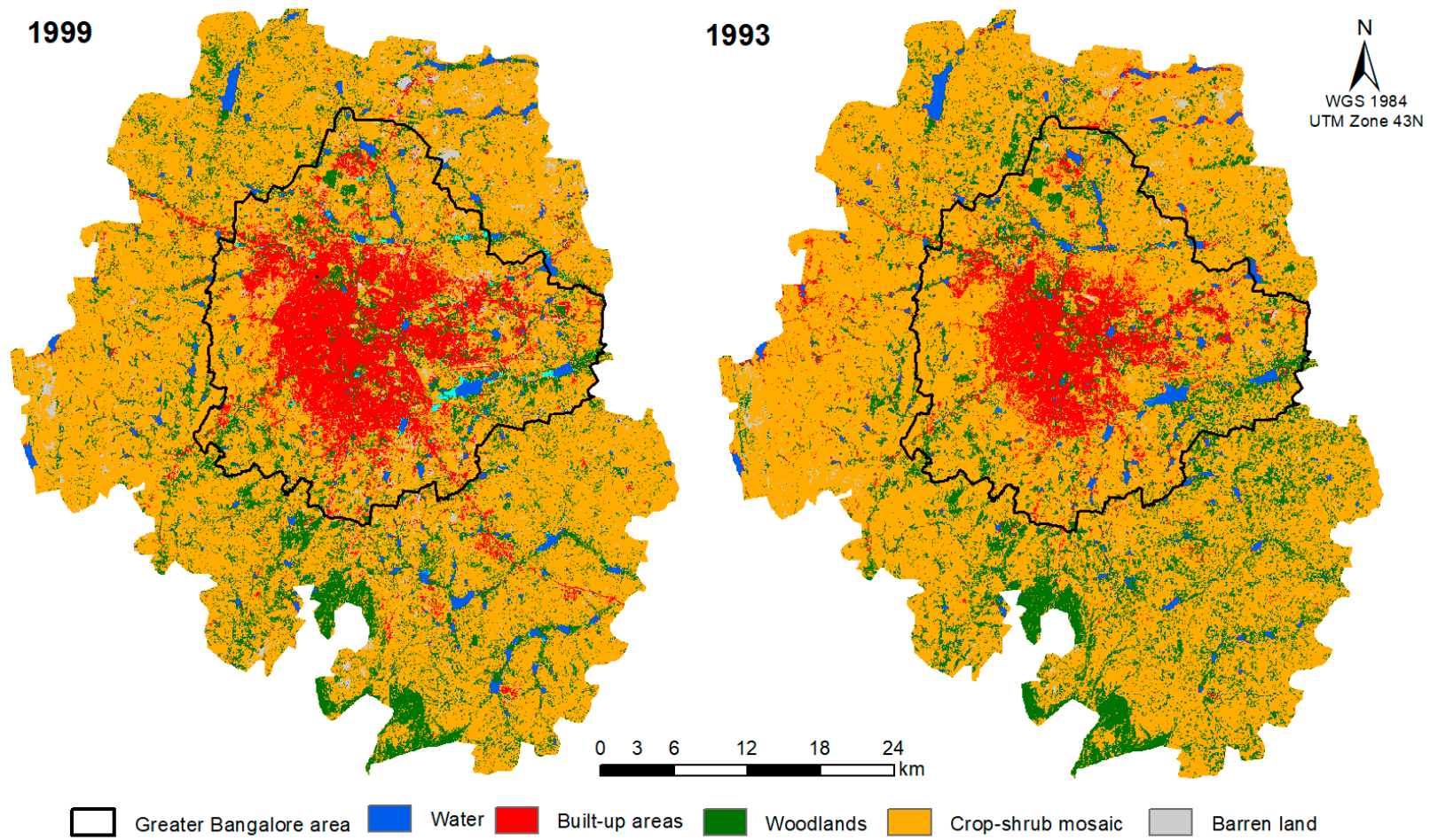
## Appendix B Land Cover Maps from 2018, 2014, 2009, 2004, 1999, 1993, 1988 and 1965 for the District Bengaluru Urban, S-India

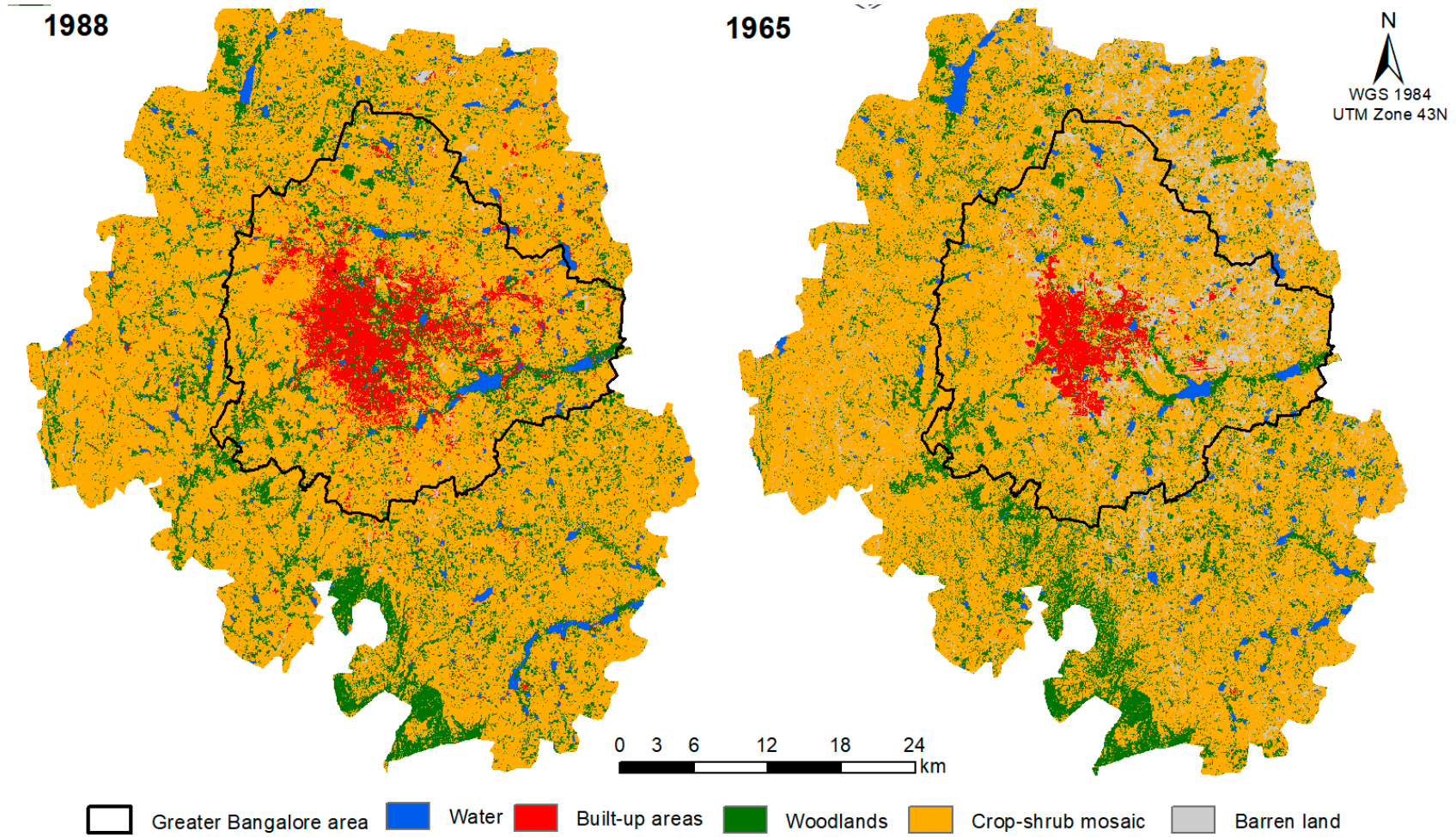


2009

2004







**Appendix C Land Cover Changes (Area in km<sup>2</sup> and Proportion in %) from 1965 to 2018 in Greater Bangalore, S-India**

Year	Water		Built-up		Woodland		Crop–shrub mosaic		Barren land		Hydrophytic vegetation	
	km <sup>2</sup>	%	km <sup>2</sup>	%	km <sup>2</sup>	%	km <sup>2</sup>	%	km <sup>2</sup>	%	km <sup>2</sup>	%
1965	20.8	2.9	51.2	7.3	85.5	12.1	481.2	68.2	67.8	9.6	1.1	0.2
1988	15.7	2.2	112.3	15.9	106.2	15.0	463.3	65.8	7.7	1.1	1.9	0.3
1993	17.8	2.5	146.0	20.7	94.8	13.4	442.7	62.7	5.1	0.7	3.4	0.5
1999	14.8	2.1	214.7	30.4	91.0	12.9	356.2	50.4	24.9	3.5	4.7	0.7
2004	14.1	2.0	287.6	40.7	58.3	8.3	296.1	41.9	44.9	6.4	5.2	0.7
2009	11.6	1.6	372.1	52.4	51.3	7.3	229.8	32.5	34.7	4.9	6.8	0.9
2014	10.6	1.5	372.5	52.7	60.9	8.6	178.7	25.3	39.2	5.6	10.4	1.5
2018	12.5	1.8	446.3	63.2	55.0	7.8	161.1	22.8	26.5	3.8	4.7	0.7

## References

- Gibbs, J.P. Wetland Loss and Biodiversity Conservation. *Conserv. Biol.* **2000**, *14*, 314–317. [[CrossRef](#)]
- Kayranli, B.; Scholz, M.; Mustafa, A.; Hedmark, Å. Carbon Storage and Fluxes within Freshwater Wetlands: A Critical Review. *Wetlands* **2010**, *30*, 111–124. [[CrossRef](#)]
- Mitsch, W.J.; Gosselink, J.G. The value of wetlands: Importance of scale and landscape setting. *Ecol. Econ.* **2000**, *35*, 25–33. [[CrossRef](#)]
- Bassi, N.; Kumar, M.D.; Sharma, A.; Pardha-Saradhi, P. Status of wetlands in India: A review of extent, ecosystem benefits, threats and management strategies. *J. Hydrol.* **2014**, *2*, 1–19. [[CrossRef](#)]
- Keddy, P. *Wetland Ecology: Principles and Conservation*, 2nd ed.; 5th printing ed.; Cambridge University Press: Cambridge, UK, 2016.
- Lang, M.W.; Tiner, R.W.; Klemas, V. *Remote Sensing of Wetlands: Applications and Advances*; CRC Press Taylor & Francis Group: Boca Raton, FL, USA, 2015.
- Feyisa, G.L.; Meilby, H.; Fensholt, R.; Proud, S.R. Automated Water Extraction Index: A new technique for surface water mapping using Landsat imagery. *Remote Sens. Environ.* **2014**, *140*, 23–35. [[CrossRef](#)]
- Mitsch, W.J.; Gosselink, J.G. *Wetlands*; John Wiley & Sons Ltd.: Chichester, UK, 2015.
- Ramsar Convention on Wetlands. Ramsar Fact Sheet 3 Wetlands: A Global Disappearing Act. 2015. Available online: [https://www.ramsar.org/sites/default/files/documents/library/factsheet3\\_global\\_disappearing\\_act\\_0.pdf](https://www.ramsar.org/sites/default/files/documents/library/factsheet3_global_disappearing_act_0.pdf) (accessed on 11 January 2019).
- Li, Y.; Zhu, X.; Sun, X.; Wang, F. Landscape effects of environmental impact on bay-area wetlands under rapid urban expansion and development policy: A case study of Lianyungang, China. *Landsc. Urban Plan.* **2010**, *94*, 218–227. [[CrossRef](#)]
- He, C.; Tian, J.; Shi, P.; Hu, D. Simulation of the spatial stress due to urban expansion on the wetlands in Beijing, China using a GIS-based assessment model. *Landsc. Urban Plan.* **2011**, *101*, 269–277. [[CrossRef](#)]
- Nagendra, H.; Gopal, D. Tree diversity, distribution, history and change in urban parks: Studies in Bangalore, India. *Urban Ecosyst.* **2011**, *14*, 211–223. [[CrossRef](#)]
- Hettiarachchi, M.; Morrison, T.H.; Wickramasinghe, D.; Mapa, R.; Alwis, A.; de McAlpine, C.A. The eco-social transformation of urban wetlands: A case study of Colombo, Sri Lanka. *Landsc. Urban Plan.* **2014**, *132*, 55–68. [[CrossRef](#)]
- Burgin, S.; Franklin, M.J.M.; Hull, L. Wetland losses in the transition to urbanization: A case study from Western Sydney, Australia. *Wetlands* **2016**, *36*, 985–994. [[CrossRef](#)]
- Iniesta-Arandia, I.; García-Llorente, M.; Aguilera, P.A.; Montes, C.; Martín-López, B. Socio-cultural valuation of ecosystem services: Uncovering the links between values, drivers of change, and human well-being. *Ecol. Econ.* **2014**, *108*, 36–48. [[CrossRef](#)]
- Andersson, E.; Nykvist, B.; Malinga, R.; Jaramillo, F.; Lindborg, R. A social-ecological analysis of ecosystem services in two different farming systems. *AMBIO* **2015**, *44* (Suppl. S1), 102–112. [[CrossRef](#)] [[PubMed](#)]
- Kansiime, F.; Kateyo, E.; Oryem-Origa, H.; Mucunguzi, P. Nutrient status and retention in pristine and disturbed wetlands in Uganda: Management implications. *Wetl. Ecol. Manag.* **2007**, *15*, 453–467. [[CrossRef](#)]
- Ehrenfeld, J.G. Exotic invasive species in urban wetlands: Environmental correlates and implications for wetland management. *J. Appl. Ecol.* **2008**, *45*, 1160–1169. [[CrossRef](#)]
- Hettiarachchi, M.; Morrison, T.H.; McAlpine, C. Forty-three years of Ramsar and urban wetlands. *Glob. Environ. Chang.* **2015**, *32*, 57–66. [[CrossRef](#)]
- Xian, G.; Crane, M.; Su, J. An analysis of urban development and its environmental impact on the Tampa Bay watershed. *J. Environ. Manag.* **2007**, *85*, 965–976. [[CrossRef](#)] [[PubMed](#)]
- Mondal, B.; Dolui, G.; Pramanik, M.; Maity, S.; Biswas, S.S.; Pal, R. Urban expansion and wetland shrinkage estimation using a GIS-based model in the East Kolkata Wetland, India. *Ecol. Indic.* **2017**, *83*, 62–73. [[CrossRef](#)]
- Smardon, R. *Sustaining the World's Wetlands*; Springer US: New York, NY, USA, 2009.
- Marcuse, P.; van Kempen, R. Conclusion: A Changed Spatial Order. In *Globalizing Cities: A New Spatial Order*; Marcuse, P., van Kempen, R., Eds.; Blackwell Publishers: Oxford, UK; Malden, MA, USA, 2000; pp. 249–275.
- Nagendra, H.; Bai, X.; Brondizio, E.S. The urban south and the predicament of global sustainability. *Nat. Sustain.* **2018**, *1*, 341–349. [[CrossRef](#)]
- Dasgupta, K. A city divided? Planning and urban sprawl in the eastern fringes of Calcutta. In *Indian Cities in Transition*; Shaw, A., Ed.; Orient Longman: Chennai, India, 2007.

26. Grimm, N.B.; Faeth, S.H.; Golubiewski, N.E.; Redman, C.L.; Wu, J.; Bai, X.; Briggs, J.M. Global change and the ecology of cities. *Science* **2008**, *319*, 756–760. [[CrossRef](#)]
27. Taubenböck, H.; Wegmann, M.; Roth, A.; Mehl, H.; Dech, S. Urbanization in India—Spatiotemporal analysis using remote sensing data. *Comput. Environ. Urban Syst.* **2009**, *33*, 179–188. [[CrossRef](#)]
28. Kumar, M.; Mukherjee, N.; Sharma, G.P.; Raghubanshi, A.S. Land use patterns and urbanization in the holy city of Varanasi, India: A scenario. *Environ. Monit. Assess.* **2010**, *167*, 417–422. [[CrossRef](#)] [[PubMed](#)]
29. Mathur, A.; Da Cunha, D. *Deccan Traverses: The Making of Bangalore's Terrain*; Rupa & Co, Rupa Publications India Pvt., Ltd.: Kolkata, India, 2006; p. 231. ISBN 9788129108524.
30. Sudha, P.; Ravindranath, N.H. A study of Bangalore urban forest. *Landsc. Urban Plan.* **2000**, *47*, 47–63. [[CrossRef](#)]
31. Sudhira, H.S.; Nagendra, H. *Local Assessment of Bangalore: Graying and Greening in Bangalore—Impacts of Urbanization on Ecosystems, Ecosystem Services and Biodiversity*; Fragkias, M., Goodness, J., Güneralp, B., Marcotullio, P.J., McDonald, R.I., Parnell, S., Schewenius, M., Sendstad, M., Seto, K.C., Wilkinson, C., et al., Eds.; Urbanization, Biodiversity and Ecosystem Services: Challenges and Opportunities: A Global Assessment; Springer: Dordrecht, The Netherlands, 2013; pp. 75–91.
32. Awuah, K.T.; Nölke, N.; Freudenberg, M.; Diwakara, B.N.; Tewari, V.P.; Kleinn, C. Spatial resolution and landscape structure along an urban-rural gradient: Do they relate to remote sensing classification accuracy?—A case study in the megacity of Bengaluru, India. *Remote Sens. Appl. Soc. Environ.* **2018**, *12*, 89–98. [[CrossRef](#)]
33. Nagendra, H.; Nagendran, S.; Paul, S.; Pareeth, S. Graying, greening and fragmentation in the rapidly expanding Indian city of Bangalore. *Landsc. Urban Plan.* **2012**, *105*, 400–406. [[CrossRef](#)]
34. Sun, F.; Sun, W.; Chen, J.; Gong, P. Comparison and improvement of methods for identifying waterbodies in remotely sensed imagery. *Int. J. Remote Sens.* **2012**, *33*, 6854–6875. [[CrossRef](#)]
35. Rebelo, L.-M.; Finlayson, C.M.; Nagabhatla, N. Remote sensing and GIS for wetland inventory, mapping and change analysis. *J. Environ. Manag.* **2009**, *9*, 2144–2153. [[CrossRef](#)]
36. Adam, E.; Mutanga, O.; Rugege, D. Multispectral and hyperspectral remote sensing for identification and mapping of wetland vegetation: A review. *Wetl. Ecol. Manag.* **2010**, *18*, 281–296. [[CrossRef](#)]
37. Chen, L.; Jin, Z.; Michishita, R.; Cai, J.; Yue, T.; Chen, B.; Xu, B. Dynamic monitoring of wetland cover changes using time-series remote sensing imagery. *Ecol. Inform.* **2014**, *24*, 17–26. [[CrossRef](#)]
38. Lv, J.; Jiang, W.; Wang, W.; Wu, Z.; Liu, Y.; Wang, X.; Li, Z. Wetland loss identification and evaluation based on landscape and remote sensing indices in Xiong'an New Area. *Remote Sens.* **2019**, *11*, 2834. [[CrossRef](#)]
39. Berhane, T.M.; Lane, C.R.; Wu, Q.; Anenkhonov, O.A.; Chepinoga, V.V.; Autrey, B.C.; Liu, H. Comparing pixel- and object-based approaches in effectively classifying wetland-dominated landscapes. *Remote Sens.* **2018**, *10*, 46. [[CrossRef](#)]
40. Niering, W.A. *Wetlands (Audubon Society Nature Guides)*; A Chanticleer Press, Ed.; National Audubon Society: New York, NY, USA, 1985; ISBN 0394731476.
41. Wu, Q. GIS and Remote Sensing Applications in Wetland Mapping and Monitoring. In *Comprehensive Geographic Information Systems*; Huang, B., Ed.; Elsevier Science: Saint Louis, MI, USA, 2017; pp. 140–157.
42. Ozesmi, S.L.; Bauer, M.E. Satellite remote sensing of wetlands. *Wetl. Ecol. Manag.* **2002**, *10*, 381–402. [[CrossRef](#)]
43. Wang, X.; Ning, L.; Yu, J.; Xiao, R.; Li, T. Changes of urban wetland landscape pattern and impacts of urbanization on wetland in Wuhan City. *Chin. Geogr. Sci.* **2008**, *18*, 47–53. [[CrossRef](#)]
44. Gautam, V.K.; Gaurav, P.K.; Murugan, P.; Annadurai, M. Assessment of surface water dynamics in Bangalore using WRI, NDWI, MNDWI, supervised classification and K-T transformation. *Aquat. Procedia* **2015**, *4*, 739–746. [[CrossRef](#)]
45. Wang, X.; Ling, F.; Yao, H.; Liu, Y.; Xu, S. Unsupervised sub-pixel water body mapping with Sentinel-3 OLCI image. *Remote Sens.* **2019**, *11*, 327. [[CrossRef](#)]
46. Acharya, T.D.A.; Subedi, A.; Lee, D.H. Evaluation of Machine Learning Algorithms for Surface Water Extraction in a Landsat 8 Scene of Nepal. *Sensors* **2019**, *19*, 2769. [[CrossRef](#)] [[PubMed](#)]
47. Yao, F.; Wang, C.; Dong, D.; Luo, J.; Shen, Z.; Yang, K. High-Resolution Mapping of Urban Surface Water Using ZY-3 Multi-Spectral Imagery. *Remote Sens.* **2015**, *7*, 12336–12355. [[CrossRef](#)]
48. Jiang, H.; Feng, M.; Zhu, Y.; Lu, N.; Huang, J.; Xiao, T. An automated method for extracting rivers and lakes from Landsat imagery. *Remote Sens.* **2014**, *6*, 5067–5089. [[CrossRef](#)]

49. Knight, J.; Corcoran, J.; Rampi, L.; Pelletier, K. Theory and Applications of Object-Based Image Analysis and Emerging Methods in Wetland Mapping. In *Remote sensing of Wetlands: Applications and Advances*; Tiner, R.W., Lang, M., Klemas, V., Eds.; CRC Press Taylor & Francis Group: Boca Raton, FL, USA, 2015; pp. 175–194. [[CrossRef](#)]
50. Mui, A.; He, Y.; Weng, Q. An object-based approach to delineate wetlands across landscapes of varied disturbance with high spatial resolution satellite imagery. *ISPRS J. Photogramm. Remote Sens.* **2015**, *109*, 30–46. [[CrossRef](#)]
51. Hu, T.; Liu, J.; Zheng, G.; Li, Y.; Xie, B. Quantitative assessment of urban wetland dynamics using high spatial resolution satellite imagery between 2000 and 2013. *Nat. Sci. Rep.* **2018**, *8*, 7409. [[CrossRef](#)]
52. D'Souza, R. *A Study on Bellandur Tank and Changes Due to Urbanisation*; A CASUMM Publication: Bangalore, India, 2007.
53. D'Souza, R.; Nagendra, H. Changes in public commons as a consequence of urbanization: The Agara lake in Bangalore, India. *Environ. Manag.* **2011**, *47*, 840–850. [[CrossRef](#)]
54. Ramachandra, T.V.; Kumar, U. Wetlands of Greater Bangalore, India: Automatic Delineation through Pattern Classifiers. *Electron. Green J.* **2008**, *1*. Available online: <https://escholarship.org/uc/item/3dp0q8f2> (accessed on 15 January 2019).
55. Bharath, H.A.; Vinay, S.; Chandan, M.C.; Gouri, B.A.; Ramachandra, T.V. Green to gray: Silicon Valley of India. *J. Environ. Manag.* **2018**, *206*, 1287–1295. [[CrossRef](#)] [[PubMed](#)]
56. Nair, J. *The Promise of the Metropolis: Bangalore's Twentieth Century*; Oxford Univ. Press: New Delhi, India, 2005.
57. Sudhira, H.S.; Ramachandra, T.V.; Subrahmanya, M.B. Bangalore. *Cities* **2007**, *24*, 379–390. [[CrossRef](#)]
58. Srinivasan, V.; Thompson, S.; Madhyastha, K.; Penny, G.; Jeremiah, K.; Lele, S. Why is the Arkavathy River drying? A multiple-hypothesis approach in a data-scarce region. *Hydrol. Earth Syst. Sci.* **2015**, *19*, 1905–1917. [[CrossRef](#)]
59. Prasad, C.S.; Anandan, S.; Gowda, N.K.S.; Schlecht, E.; Buerkert, A. Managing nutrient flows in Indian urban and peri-urban livestock systems. *Nutr. Cycl. Agroecosyst.* **2019**, *115*, 159–172. [[CrossRef](#)]
60. Pani, N. Resource cities across phases of globalization: Evidence from Bangalore. *Habitat Int.* **2009**, *33*, 114–119. [[CrossRef](#)]
61. Smitha, K.C. *Urban Governance and Bangalore Water Supply & Sewerage Board (BWSSB)*; Institute of Social and Economic Change: Bangalore, India, 2006.
62. CLC (Centre for Lake Conservation). EMPRI (Environmental Management and Policy Research Institute) Draft Report on Inventorisation of Water Bodies in Bengaluru Metropolitan Area (BMA). Department of Forest, Ecology and Environment, Government of Karnataka, India. Available online: [http://www.nrs.fs.fed.us/pubs/gtr/gtr\\_nc245.pdf](http://www.nrs.fs.fed.us/pubs/gtr/gtr_nc245.pdf) (accessed on 11 November 2018).
63. BBMP. *Namma Bangalore Nisarga: An Action Plan for Development of Bangalore's Lakes*; Bruhat Bangalore Mahanagara Palike (BBMP): Bangalore, India, 2010.
64. Nagendra, H.; Gopal, D. Street trees in Bangalore: Density, diversity, composition and distribution. *Urban For. Urban Green.* **2010**, *9*, 129–137. [[CrossRef](#)]
65. Chander, G.; Markham, B.L.; Helder, D.L. Summary of current radiometric calibration coefficients for Landsat MSS, TM, ETM+, and EO-1 ALI sensors. *Remote Sens. Environ.* **2009**, *113*, 893–903. [[CrossRef](#)]
66. Chavez, P.S., Jr. Image-based atmospheric corrections-revisited and improved photogrammetric engineering and remote sensing. *Photogramm. Eng. Remote Sens.* **1996**, *62*, 1025–1036.
67. Dashora, A.; Lohani, B.; Malik, J.N. A repository of earth resource information—CORONA satellite programme. *Curr. Sci.* **2007**, *92*, 926–932.
68. Van, T.T.; Duong, P.; Nasahara, K. How does land use/land cover map's accuracy depend on number of classification classes? *Sci. Online Lett. Atmos.* **2019**, *15*, 28–31.
69. Anderson, J.R.; Hardy, E.E.; Roach, J.T.; Witmer, R.E. *Land Use and Land Cover Classification Systems for Use with Remote Sensor Data*; Professional Paper 964; Geological Service: Washington, DC, USA, 1976.
70. Cadenasso, M.L.; Pickett, S.T.A.; Grove, J.M. Dimensions of ecosystem complexity: Heterogeneity, connectivity, and history. *Ecol. Complex.* **2006**, *3*, 1–12. [[CrossRef](#)]
71. Cadenasso, M.L.; Pickett, S.T.A.; Schwarz, K. Spatial heterogeneity in urban ecosystems: Reconceptualizing land cover and a framework for classification. *Front. Ecol. Environ.* **2007**, *5*, 80–88. [[CrossRef](#)]
72. Hawken, S.; Metternicht, G.; Chang, C.W.; Liew, S.C.; Gupta, A. Remote Sensing of Urban Ecological Infrastructure in Desakota Environments: A review of current approaches. In Proceedings of the 35th Asian Conference on Remote Sensing (ACRS 2014), Nay Pyi Taw, Myanmar; Available online: <https://doi.org/10.13140/2.1.3202.9768> (accessed on 10 October 2019).

73. Fukunaga, K.; Hostetler, L. The estimation of the gradient of a density function, with applications in pattern recognition. *IEEE Trans. Inf. Theory* **1975**, *21*, 32–40. [[CrossRef](#)]
74. Comaniciu, D.; Meer, P. Mean shift: A robust approach toward feature space analysis. *IEEE Trans. Pattern Anal. Mach. Intell.* **2002**, *24*, 603–619. [[CrossRef](#)]
75. Breiman, L. Random forests. *Mach. Learn.* **2001**, *45*, 5–32. [[CrossRef](#)]
76. Corredor, X. AcAtaMa QGIS Plugin (Version 19.11.21). SMBByC-IDEAM. Available online: <https://smbbyc.bitbucket.io/qgisplugins/acatama> (accessed on 20 November 2019).
77. QGIS Development Team. QGIS Geographic Information System. Open Source Geospatial Foundation. Available online: <http://qgis.org> (accessed on 6 June 2018).
78. Cochran, W.G. *Sampling Techniques*, 3rd ed.; John Wiley & Sons: New York, NY, USA, 1977.
79. Congalton, R.G.; Green, K. *Assessing the Accuracy of Remotely Sensed Data: Principles and Practices*, 2nd ed.; CRC Press: Boca Raton, FL, USA, 2009.
80. Olofsson, P.; Foody, G.M.; Herold, M.; Stehman, S.V.; Woodcock, C.E.; Wulder, M.A. Good practices for estimating area and assessing accuracy of land change. *Remote Sens. Environ.* **2014**, *148*, 42–57. [[CrossRef](#)]
81. Pontius, R.G.; Millones, M. Death to Kappa: Birth of quantity disagreement and allocation disagreement for accuracy assessment. *Int. J. Remote Sens.* **2011**, *32*, 4407–4429. [[CrossRef](#)]
82. Hoffmann, E.; Jose, M.; Nölke, N.; Möckel, T. Construction and use of a simple index of urbanisation in the rural–urban interface of Bangalore, India. *Sustainability* **2017**, *9*, 2146. [[CrossRef](#)]
83. Schlesinger, J. Agriculture along the Urban–Rural Continuum: A GIS-based Analysis of Spatiotemporal Dynamics in Two Medium-Sized AFRICAN cities. *Freibg. Geogr. Hefte* **2013**, *70*. Available online: <https://www.geographie.uni-freiburg.de/publikationen/abstracts/fgh70-en> (accessed on 10 January 2019).
84. Schneider, A.; Woodcock, C.E. Compact, dispersed, fragmented, extensive? A comparison of urban growth in twenty-five global cities using remotely sensed data, pattern metrics and census information. *Urban Stud.* **2008**, *45*, 659–692. [[CrossRef](#)]
85. Thapa, R.; Murayama, Y. Examining spatiotemporal urbanization patterns in Kathmandu Valley, Nepal: Remote sensing and spatial metrics approaches. *Remote Sens.* **2009**, *1*, 534–556. [[CrossRef](#)]
86. Wu, Q.; Li, H.; Wang, R.; Paulussen, J.; He, Y.; Wang, M.; Wang, B.; Wang, Z. Monitoring and predicting land use change in Beijing using remote sensing and GIS. *Landsc. Urban Plan.* **2006**, *78*, 322–333. [[CrossRef](#)]
87. Vaz, E. Managing urban coastal areas through landscape metrics: An assessment of Mumbai’s mangrove system. *Ocean Coast. Manag.* **2014**, *98*, 27–37. [[CrossRef](#)]
88. Chandrashekar, J.S.; Babu, K.L.; Somashekar, R.K. Impact of urbanization on Bellandur Lake, Bangalore—A case study. *J. Environ. Biol.* **2003**, *24*, 223–227. [[PubMed](#)]
89. Jumbe, A.S.; Nandini, N. Heavy metals analysis and sediment quality values in urban lakes. *Am. J. Environ. Sci.* **2009**, *5*, 678–687. [[CrossRef](#)]
90. National Geographic. Why This Lake Keeps Catching on Fire. Available online: <https://news.nationalgeographic.com/2018/02/bangalore-india-lake-bellandur-catches-fire-pollution/> (accessed on 2 February 2019).
91. Buchanan, F. *A Journey from Madras through the Countries of Mysore, Canara, and Malabar*; Cambridge University Press: New-York, NY, USA, 2011.
92. Murphy, A.; Johan, P.; Enqvist, J.P.; Tengö, M. Place-making to transform urban social–ecological systems: Insights from the stewardship of urban lakes in Bangalore, India. *Sustain. Sci.* **2019**, *14*, 607–623. [[CrossRef](#)]
93. Nagendra, H.; Sudhira, H.S.; Katti, M.; Schewenius, M. Sub-regional Assessment of India: Effects of Urbanization on Land Use, Biodiversity and Ecosystem Services. In *Urbanization, Biodiversity and Ecosystem Services: Challenges and Opportunities: A Global Assessment*; Fragkias, M., Goodness, J., Güneralp, B., Marcotullio, P.J., McDonald, R.I., Parnell, S., Schewenius, M., Sendstad, M., Seto, K.C., Wilkinson, C., Eds.; Springer: Dordrecht, The Netherlands, 2013; pp. 65–74.
94. Baud, I.S.A.; de Wit, J. *New Forms of Urban Governance in India: Shifts, Models, Networks and Contestations*; SAGE Publications: Thousand Oaks, CA, USA, 2009.
95. Singh, A. Digital change detection techniques using remotely-sensed data. *Int. J. Remote Sens.* **1989**, *10*, 989–1003. [[CrossRef](#)]
96. Coppin, P.; Jonckheere, I.; Nackaerts, K.; Muys, B.; Lambin, E. Digital change detection methods in ecosystem monitoring: A review. *Int. J. Remote Sens.* **2004**, *25*, 1565–1596. [[CrossRef](#)]

97. Ruelland, D.; Tribotté, A.; Puech, C.; Dieulin, C. Comparison of methods for LUCC monitoring over 50 years from aerial photographs and satellite images in a Sahelian catchment. *Int. J. Remote Sens.* **2011**, *32*, 1747–1777. [[CrossRef](#)]
98. Vermaat, J.E.; Goosen, H.; Omtzigt, N. Do biodiversity patterns in Dutch wetland complexes relate to variation in urbanisation, intensity of agricultural land use or fragmentation. In *Biodiversity and Conservation in Europe*; Hawksworth, D.L., Bull, A.T., Eds.; Springer: Dordrecht, The Netherland, 2007; pp. 343–353.



© 2020 by the authors. Licensee MDPI, Basel, Switzerland. This article is an open access article distributed under the terms and conditions of the Creative Commons Attribution (CC BY) license (<http://creativecommons.org/licenses/by/4.0/>).